

# Nonzero $\theta_{13}$ and Leptogenesis in a Type-I See-saw Model with $A_4$ Symmetry

Biswajit Karmakar<sup>a,1</sup>, Arunansu Sil<sup>a,2</sup>

<sup>a</sup> *Indian Institute of Technology Guwahati, 781039 Assam, India*

## Abstract

In the light of recent discovery of nonzero  $\theta_{13}$ , we have analyzed the Altarelli-Feruglio  $A_4$  flavor symmetry model extended with additional flavon. The inclusion of the new field leads to the deviation from exact tri-bimaximal neutrino mixing pattern in the context of type-I see-saw by producing a nonzero  $\theta_{13}$  consistent with the recent experimental results at the leading order. A sum rule for light neutrino masses is also obtained in this context. The set-up constraints the two Majorana phases involved in the lepton mixing matrix in terms of  $A_4$  parameter space. We have shown that a nonzero lepton asymmetry can be generated while next-to-leading order contributions to the neutrino Yukawa couplings are considered. The two Majorana phases play crucial role in CP-asymmetry parameter and the involvement of  $\theta_{13}$  in it, is exercised.

---

<sup>1</sup>k.biswajit@iitg.ernet.in

<sup>2</sup>asil@iitg.ernet.in

# 1 Introduction

The evidence of non-vanishing value of the mixing angle  $\theta_{13}$  from several experiments (Double Chooz [1], Daya Bay [2], RENO [3], T2K [4]), receives particular attention in these days since the precise determination of neutrino mixing would be crucial for better understanding the issues related to the flavor. In this context it is important to study the neutrino mass matrix,  $m_\nu$ , that can be structured from discrete flavor symmetry. The neutrino mass matrix  $m_\nu$ , in general, can be diagonalized by the  $U_{PMNS}$  matrix (in the basis where charged leptons are diagonal) as

$$m_\nu = U_{PMNS}^* \text{diag}(m_1, m_2, m_3) U_{PMNS}^\dagger, \quad (1.1)$$

where  $m_1, m_2, m_3$  are the real mass eigenvalues. The standard parametrization [5] of the  $U_{PMNS}$  matrix is given by

$$U_{PMNS} = \begin{bmatrix} c_{12}c_{13} & s_{12}c_{13} & s_{13}e^{-i\delta} \\ -s_{12}c_{23} - c_{12}s_{13}s_{23}e^{i\delta} & c_{12}c_{23} - s_{12}s_{13}s_{23}e^{i\delta} & c_{13}s_{23} \\ s_{12}s_{23} - c_{12}s_{13}c_{23}e^{i\delta} & -c_{12}s_{23} - s_{12}s_{13}c_{23}e^{i\delta} & c_{13}c_{23} \end{bmatrix} \begin{bmatrix} 1 & 0 & 0 \\ 0 & e^{i\alpha_{21}/2} & 0 \\ 0 & 0 & e^{i\alpha_{31}/2} \end{bmatrix}, \quad (1.2)$$

where  $c_{ij} = \cos \theta_{ij}$ ,  $s_{ij} = \sin \theta_{ij}$ ,  $\delta$  is the CP-violating Dirac phase while  $\alpha_{21}$  and  $\alpha_{31}$  are the two CP-violating Majorana phases. Though the neutrino mixing angles  $\theta_{12}$ ,  $\theta_{23}$  and the two mass-squared differences have been well measured at several neutrino oscillation experiments [6], only an upper bound was present (consistent with zero) for the other mixing angle  $\theta_{13}$  till 2011 [7]. Then the recent results from Double Chooz [1], Daya Bay [2], RENO [3], T2K [4], suggest that in fact  $\theta_{13}$  is nonzero and of sizable magnitude. From the updated global analysis [8] involving all the data from neutrino experiments, we have  $1\sigma$  and  $3\sigma$  ranges of mixing angles and the mass-squared differences as mentioned (NH and IH stand for the normal and inverted mass hierarchies respectively) in Table 1. Majorana phases are not appearing in neutrino oscillation probability and therefore can not be constrained from neutrino oscillation data directly [9]. As of now, any specific constraint on the Dirac CP violating phase  $\delta$  is still missing and so it is ranged between 0 to  $2\pi$  [8].

This clearly indicates a completely different pattern of mixing in the lepton sector compared to the quark sector. Efforts therefore have been exercised for a long time in realizing the neutrino mixing pattern and among them patterns based on discrete flavor groups attract particular attention. A case of special mention is where  $\sin^2 \theta_{12} = 1/3$ ,  $\sin^2 \theta_{23} = 1/2$  along with  $\sin \theta_{13} = 0$  resulted, called the tri-bimaximal (TBM) mixing pattern [10]. Note that all these mixing angles inclusive of vanishing  $\theta_{13}$  were in the right ballpark of experimental findings before 2011. Many discrete groups have been employed [11] in realizing the TBM mixing pattern, and  $A_4$  turned out to be a special one which can reproduce this pattern in a most economic way [12–14].  $A_4$  is a discrete group of even permutations of four objects.

Oscillation parameters	$1\sigma$ range	$3\sigma$ range
$\Delta m_{21}^2$	7.42–7.79 [ $10^{-5}$ eV <sup>2</sup> ]	7.11–8.18
$ \Delta m_{31}^2 $	2.41 – 2.53 [ $10^{-3}$ eV <sup>2</sup> ] (NH)	2.30 – 2.65
	2.32 – 2.43 [ $10^{-3}$ eV <sup>2</sup> ] (IH)	2.20 – 2.54
$\sin^2 \theta_{12}$	0.307–0.339	0.278–0.375
$\sin^2 \theta_{23}$	0.439–0.599 (NH)	0.392–0.643
	0.530–0.598 (IH)	0.403–0.640
$\sin^2 \theta_{13}$	0.0214–0.0254 (NH)	0.0177–0.0294
	0.0221–0.0259 (IH)	0.0183–0.0297

Table 1: Summary of neutrino oscillation parameters for normal and inverted neutrino mass hierarchy from the analysis of [8].

It has three inequivalent one-dimensional representations ( $1, 1', 1''$ ) and a three dimensional representation (3). In this work, we mostly concentrate on Altarelli-Feruglio (AF) type of model [14] where the light neutrino masses are generated through type-I see-saw mechanism. So the right handed neutrinos ( $N^c$ ) are introduced which transform as a triplet of  $A_4$ . Flavon fields transforming trivially and non-trivially under the  $A_4$  are also introduced, whose vacuum expectation values (VEV) break the  $A_4$  flavor symmetry at some high scale. The framework is supersymmetric and based on the Standard Model (SM) gauge interactions. As it was argued in [14], the introduction of supersymmetry was instrumental to provide the correct vacuum alignment. Then the type-I see-saw leads to the TBM mixing in the light neutrinos while the charged lepton mass matrix is found to be diagonal.

However with the latest developments toward the nonzero value of  $\theta_{13}$ , it is essential to modify the exact TBM pattern. Several attempts were made in this direction during last couple of years in the context of  $A_4$ -based flavor models [15–23]. It is to be noted from these analysis that inclusion of higher order terms only would not produce a sufficiently large  $\theta_{13}$  as predicted by experiments. So a leading order deformation of the original  $A_4$  model is required which we will study in this work.

Another important phenomenon that can not be realized in the context of the Standard Model is to explain the observed matter-antimatter asymmetry of the Universe. However it is known that the standard weak interactions can lead to processes (mediated by sphalerons) which can convert the baryons and leptons. So a baryon asymmetry can be effectively generated from a lepton asymmetry. The mechanism for generating the lepton asymmetry is called leptogenesis [24]. The discussion of it is of particular importance here, while explaining the generation of light neutrino mass through type-I see-saw mechanism. The inclusion of heavy right handed (RH) neutrinos in the framework provides the opportunity to discuss also the

leptogenesis scenario through the CP-violating decay of it in the early Universe. Although the ingredients (RH neutrinos) are present, it is known that the see-saw models predicting the exact TBM structure can not generate the required lepton asymmetry [25], the reason being the term involved in the asymmetry related to the neutrino Yukawa coupling matrix is proportional to the identity matrix and thus the lepton number asymmetry parameter vanishes. However it was shown in [25] that one can in principle consider higher dimensional operators in the neutrino Yukawa couplings of the model. The effect of this inclusion is to deviate the products of the Yukawa-terms in lepton asymmetry parameter from unity and thereby generating nonzero lepton asymmetry.

In this work, our aim is to produce nonzero  $\theta_{13}$  as well as to realize leptogenesis in the same framework. We have extended the flavon-sector of AF [14] by introducing an extra flavon,  $\xi'$  which transforms as  $1'$  under  $A_4$ . Similar sort of extensions have been considered in [16, 18]. However the analyses in those works are mostly related to the deviation over the final form of  $m_\nu$  obtained from AF model, while here we consider modification of  $m_\nu$  through the deviation from the RH neutrino mass matrix  $M_R$ . In [20, 26], a perturbative deviation from tri-bimaximal mixing is considered through  $M_R$ , though leptogenesis was not considered in that framework. This provides the opportunity to analyze  $M_R$  in detail and the effect on the Majorana phases can also be studied. Inclusion of  $Z_3$  symmetry in the model forbids several unwanted terms and thus helps in constructing specific structure of the coupling matrices. While the charged lepton mass matrix is found to be in the diagonal form, the RH neutrino mass matrix has an additional structure originated from  $\xi'$ -related term. Due to this, the light neutrino diagonalizing matrix no longer remains in TBM form rather a deviation is resulted which leads to nonzero  $\theta_{13}$ . In the RH neutrino mass matrix, three complex parameters  $a, b$  and  $d$  are present. We found that the low energy observables can be expressed in terms of two parameters  $\lambda_1 (= |d/a|)$ ,  $\lambda_2 (= |b/a|)$ ; relative phase between  $b$  and  $a$  ( $\phi_{ba}$ ) and  $|a|$ . The relative phase between  $d$  and  $a$  are assumed to be zero for simplicity. We have studied the dependence of  $\theta_{13}$  on  $\lambda_1$ . The allowed range of  $\theta_{13}$  restricts the range of the parameter space of  $\lambda_1$ . Then following the analysis [27], we are able to constrain also the Majorana phases ( $\alpha_{21}, \alpha_{31}$ ) involved in the  $U_{PMNS}$  and study their dependence on the parameter  $\lambda_2$  (for this we have fixed  $\lambda_1$  to its value that corresponds to the best-fit value of  $\sin^2 \theta_{13}$ ) for both normal and inverted hierarchy cases. In this scenario, we obtain a general sum rule involving the light neutrino masses  $m_{i=1,2,3}$  and the Majorana phases,  $\alpha_{21}, \alpha_{31}$ . The effective mass parameter involved in the neutrinoless double beta decay is also estimated. We then investigate the generation of lepton asymmetry from the decay of RH neutrinos within ‘one flavor approximation’ [27–30]. As previously stated, nonzero lepton asymmetry can be obtained once we include the next to leading order terms in the Yukawa sector. Note

that this inclusion does not spoil the diagonal nature of charged lepton mass matrix. The explicit appearance of these Majorana phases in the CP-asymmetry parameter,  $\epsilon_i$ , provides the possibility of studying the dependence of  $\epsilon_i$  on  $\lambda_2$ . The expression of  $\epsilon_i$  also involves the  $\theta_{13}$  mixing angle in our set-up. Since  $\theta_{13}$  depends on  $\lambda_1$ , we have also studied the variation of  $\epsilon_i$  (or baryon asymmetry  $Y_B$ ) against  $\theta_{13}$  while  $\lambda_2$  is fixed at a suitable value.

In section 2, we describe the structure of the model by specifying the fields involved and their transformation properties under the symmetries imposed. Then in section 3, we discuss the eigenvalues and phases involved in the RH neutrino sector. We also find the lepton mixing matrix and study the correlation between the mixing angles in terms of  $\lambda_1$ . Section 4 is devoted to study the Majorana phases, light neutrino masses, effective mass parameter involved in neutrinoless double beta decay. Leptogenesis is analysed in section 5 and following that, we have conclusion in section 6.

## 2 Structure of The Model

We consider here an extension of the original Altarelli-Feruglio(AF) model [14] (with right-handed neutrinos) for generating lepton masses and mixing by introducing one additional flavon  $\xi'$  which transforms as  $1'$  under  $A_4$ . We will find this modification turns out to be instrumental to have nonzero  $\theta_{13}$ . The particle content and the symmetries of the model are provided in Table 2. The framework is supersymmetric and the gauge group is same as that of the Standard Model. All the left handed doublets  $L_{i(=1,2,3)}$  transform as  $A_4$  triplets, and the RH charged leptons  $e^c, \mu^c, \tau^c$  are  $A_4$  singlets  $1, 1'', 1'$  respectively. In order to realize the type-I see-saw, three right handed neutrinos ( $N_i^c$ ) are considered which are triplets of  $A_4$ . The flavor symmetry  $A_4$  is accompanied by a discrete  $Z_3$  symmetry, which forbids several unwanted terms. The  $A_4$  multiplication rules are mentioned in appendix A. There are four flavons ( $\phi_S, \phi_T, \xi, \xi'$ ) in the model, which are SM gauge singlets. When the flavons (the scalar component of it) get vacuum expectation values (vev),  $\langle \phi_S \rangle = (v_S, v_S, v_S)$ ,  $\langle \phi_T \rangle = (v_T, 0, 0)$ ,  $\langle \xi \rangle = u$ ,  $\langle \xi' \rangle = u'$ , the  $A_4 \times Z_3$  symmetry is broken and generates the flavor structure of the sector. The fields  $\phi_0^S, \phi_0^T$  and  $\xi_0$  are the driving fields, carrying two units of  $U(1)_R$  charges, introduced to realize the vacuum alignments of the flavon fields,  $\phi_S, \phi_T, \xi, \xi'$ . Supersymmetry helps in realizing this vacuum alignment by setting the F-term to be zero. A brief discussion on the vacuum alignment is provided in appendix B.  $H_u$  and  $H_d$  are the two Higgs doublets present in the set-up transforming as singlets under  $A_4$  with the vevs  $v_u$  and  $v_d$  respectively. With the above mentioned field configuration, the effective superpotential for the charged

	$e^c$	$\mu^c$	$\tau^c$	$L_i$	$N_i^c$	$H_u$	$H_d$	$\phi_S$	$\phi_T$	$\xi$	$\xi'$	$\phi_0^S$	$\phi_0^T$	$\xi_0$
$A_4$	1	$1''$	$1'$	3	3	1	1	3	3	1	$1'$	3	3	1
$Z_3$	$\omega$	$\omega$	$\omega$	$\omega$	$\omega^2$	1	$\omega$	$\omega^2$	1	$\omega^2$	$\omega^2$	$\omega^2$	1	$\omega^2$
$U(1)_R$	1	1	1	1	1	0	0	0	0	0	0	2	2	2

Table 2: Fields content and transformation properties under the symmetries imposed on the model. Here  $\omega$  is the third root of unity.

lepton sector contains the following terms in the leading order (LO),

$$w_L = \left[ y_e e^c (L\phi_T) + y_\mu \mu^c (L\phi_T)' + y_\tau \tau^c (L\phi_T)'' \right] \left( \frac{H_d}{\Lambda} \right), \quad (2.1)$$

where  $\Lambda$  is the cut-off scale of the theory and  $y_e, y_\mu, y_\tau$  are the coupling constants. Terms in the first parenthesis represent products of two triplets (here  $L$  and  $\phi_T$  for example) under  $A_4$ , each of these terms contracts with  $A_4$  singlets 1,  $1''$  and  $1'$  corresponding to  $e^c, \mu^c$  and  $\tau^c$  respectively. Finally it sets the charged lepton coupling matrix as the diagonal one in the leading order,

$$Y_L = \frac{v_T}{\Lambda} \begin{bmatrix} y_e & 0 & 0 \\ 0 & y_\mu & 0 \\ 0 & 0 & y_\tau \end{bmatrix}, \quad (2.2)$$

once the flavon vevs as well as the Higgs vevs are inserted. The relative hierarchies between the charged leptons can be generated if one introduces global Froggatt-Nielsen ( $U(1)_{FN}$ ) flavor symmetry, under which RH charged leptons have different charges in addition to a FN field [31, 32].

In absence of the  $\xi'$  field, the neutrino sector would have the superpotential of the form

$$w_\nu = y(N^c L)H_u + x_A \xi(N^c N^c) + x_B(N^c N^c \phi_S), \quad (2.3)$$

which yields the Dirac ( $m_D$ ) and Majorana ( $M_R$ ) neutrino mass matrices at the LO as given by

$$m_D = y v_u \begin{bmatrix} 1 & 0 & 0 \\ 0 & 0 & 1 \\ 0 & 1 & 0 \end{bmatrix} \equiv Y_{\nu 0} v_u; \quad M_R = \begin{bmatrix} a + 2b/3 & -b/3 & -b/3 \\ -b/3 & 2b/3 & a - b/3 \\ -b/3 & a - b/3 & 2b/3 \end{bmatrix}, \quad (2.4)$$

where  $a = 2x_A v_u, b = 2x_B v_S$  and  $Y_{\nu 0}$  can be taken as the LO neutrino Yukawa coupling matrix. Here  $y, x_A$ , and  $x_B$  are respective coupling constants. It has been known [12–14] that this kind of structure produces the exact TBM mixing, predicting  $\theta_{13} = 0$ . However in

our setup, the inclusion of  $\xi'$  ensures the presence of another term in the superpotential  $w_\nu$ , given by

$$x_N \xi' (N^c N^c), \quad (2.5)$$

at the LO, where  $x_N$  is another coupling constant. It introduces a modified Majorana mass matrix, compared to the one ( $M_R$ ) in TBM case, having the form

$$M_{Rd} = \begin{bmatrix} a + 2b/3 & -b/3 & -b/3 \\ -b/3 & 2b/3 & a - b/3 \\ -b/3 & a - b/3 & 2b/3 \end{bmatrix} + \begin{bmatrix} 0 & 0 & d \\ 0 & d & 0 \\ d & 0 & 0 \end{bmatrix}, \quad (2.6)$$

where  $d = 2x_N u'$ . Since this additional term is also at the renormalizable level, we expect the term  $d$  to be of the order of  $a$  and  $b$ , in general. Inclusion of higher order terms in  $m_D$  would be very important in having leptogenesis as we will discuss it in section 5.

In general we expect the vevs of the flavon fields ( $v_S, v_T, u, u'$ ) are of same order of magnitude  $\sim v$  (say). Therefore, the magnitude of light neutrino  $m_\nu$  becomes  $\sim (yv_u)^2/v$ , generated through type-I see-saw mechanism. However there could be operators like  $(LH_u)(LH_u)$ , which can also contribute to the light neutrino mass. In our model such terms appear only in combination with  $\phi_S, \xi$  and  $\xi'$  in quadrature  $(LH_u LH_u \frac{1}{\Lambda^3} [\phi_S^2, \phi_S \xi, \phi_S \xi', \xi \xi', \xi'^2])$ , as  $LH_u LH_u$  is not an invariant under  $Z_3$ . Note that these terms contribute to the light neutrino mass of order  $\frac{v^2}{v} \kappa^3$  where  $\kappa = \frac{v}{\Lambda} \ll 1$ . Hence they are relatively small compared to the neutrino mass generated from type-I see-saw by order of  $\kappa^3$  with  $y \sim \mathcal{O}(1)$  or so and therefore can be neglected in the subsequent analysis.

There are next-to-leading order (NLO) corrections present in the model which are suppressed by  $1/\Lambda^n$  with  $n \geq 1$ . For the charged lepton, the leading order (LO) contribution  $f^c(L\phi_T) \frac{H_d}{\Lambda}$  ( $f^c = e^c, \tau^c, \mu^c$ ), is already  $1/\Lambda$  suppressed. So possible NLO contributions are  $f^c(L(\phi_T \phi_T)_A) \frac{H_d}{\Lambda^2}$  and  $f^c(L(\phi_T \phi_T)_S) \frac{H_d}{\Lambda^2}$ , where the suffixes  $A$  and  $S$  stand for anti-symmetric and symmetric triplet components from the product of two triplets in the first parenthesis under  $A_4$ . Now the first term essentially vanishes from the direction of vevs of  $\phi_T$  and the contribution coming from the second term is again diagonal, similar to the one obtained from LO term. So a mere redefinition of  $y_e, y_\mu, y_\nu$  would keep the charged lepton matrix as a diagonal, even if NLO contributions are incorporated. This conclusion is in line of earlier observation [14, 25].

We could as well include higher order terms involving  $1/\Lambda$  (which are allowed by all the symmetries imposed) to the neutrino Yukawa coupling as  $x_C(N^c L)_S \phi_T H_u / \Lambda + x_D(N^c L)_A \phi_T H_u / \Lambda$ , with  $x_C$  and  $x_D$  as coupling constants. Therefore, at the next-to-leading order, the neutrino

Yukawa coupling matrix can be re-written as,

$$\begin{aligned}
Y_\nu &= Y_{\nu 0} + \delta Y_\nu \\
&= y \begin{bmatrix} 1 & 0 & 0 \\ 0 & 0 & 1 \\ 0 & 1 & 0 \end{bmatrix} + \frac{x_C v_T}{\Lambda} \begin{bmatrix} 2 & 0 & 0 \\ 0 & 0 & -1 \\ 0 & -1 & 0 \end{bmatrix} + \frac{x_D v_T}{\Lambda} \begin{bmatrix} 0 & 0 & 0 \\ 0 & 0 & -1 \\ 0 & 1 & 0 \end{bmatrix}.
\end{aligned} \tag{2.7}$$

This will not produce any significant effect on the light neutrino masses and mixing obtained through type-I see-saw mechanism primarily with leading order  $m_D$  and  $M_{Rd}$ , as those terms are suppressed by the cut-off scale  $\Lambda$  compared to the LO contribution. However these will have important role in leptogenesis, what we will discuss in section 5.

For RH Majorana neutrinos, the non-vanishing NLO corrections in the mass matrix arise from the following terms

$$\begin{aligned}
\delta M_{Rd} &= C_1(N^c N^c)_S \phi_T \xi / \Lambda + C_2(N^c N^c)_A \phi_T \xi' / \Lambda + C_3(N^c N^c)(\phi_S \phi_T) / \Lambda \\
&+ C_4(N^c N^c)''(\phi_S \phi_T)' / \Lambda + C_5(N^c N^c)'(\phi_S \phi_T)'' / \Lambda \\
&+ C_6(N^c N^c)_S(\phi_S \phi_T)_S / \Lambda + C_7(N^c N^c)_S(\phi_S \phi_T)_A / \Lambda.
\end{aligned} \tag{2.8}$$

Here  $C_{i=1,\dots,7}$  are the respective couplings and prefixes ' and '' correspond to the 1' and 1'' singlets of  $A_4$  produced from the multiplication of two triplets under  $A_4$  within (...). Terms proportional to  $C_3$  and  $C_4$  can be absorbed in  $M_{Rd}$  and contributions from the remaining terms produce a deviation from  $M_{Rd}$  that can be written in a compact form as

$$\Delta M_{Rd} = \begin{bmatrix} 2X_D & X_B & -X_A \\ X_B & 2X_A & X_D \\ -X_A & X_D & X_B \end{bmatrix},$$

where  $X_D = (3C_6 v_s + C_7 v_s + C_1 u) \kappa$ ,  $X_B = C_5 v_s \kappa$  and  $X_A = (2C_7 v_s + C_2 u_N) \kappa$ . Almost similar type of conclusion was obtained in [27], apart from the fact that we have absorbed the term proportional to  $C_4$  in LO contribution of  $M_{Rd}$  and a new contribution coming from  $C_2$  (through  $\xi'$ ) is included in the definition of  $X_A$ .

### 3 Neutrino Masses and Mixing

Light neutrino mass matrix is obtained through the type-I see-saw mechanism as  $m_\nu = m_D^T M^{-1} m_D$ , where  $M$  is the Majorana mass matrix for RH neutrinos. Note that the Majorana mass matrix  $M$ , with the form  $M_R$  as in Eq.(2.4) (*i.e.* without  $\xi'$  field), can be diagonalized through  $U_{TB}^T M_R U_{TB} = \text{diag}(M_{R1} e^{i\phi_1}, M_{R2} e^{i\phi_2}, M_{R3} e^{i\phi_3})$ , where  $U_{TB}$  exhibits



the TBM mixing pattern [10] and is described by,

$$U_{TB} = \begin{bmatrix} \sqrt{\frac{2}{3}} & \frac{1}{\sqrt{3}} & 0 \\ -\frac{1}{\sqrt{6}} & \frac{1}{\sqrt{3}} & \frac{1}{\sqrt{2}} \\ -\frac{1}{\sqrt{6}} & \frac{1}{\sqrt{3}} & -\frac{1}{\sqrt{2}} \end{bmatrix}, \quad (3.1)$$

and  $M_{R1,2,3}$  are given by  $|b + a|$ ,  $|a|$  and  $|b - a|$  respectively.  $\phi_{1,2,3}$  are the arguments of the eigenvalues respectively. It is found [20] that the light neutrino mass matrix  $m_\nu$  ( $= m_D^T M_R^{-1} m_D$ ) in this case can also be diagonalized by a matrix  $U$  which is same as  $U_{TB}$  except the second and third rows of it are interchanged (apart from the phases involved), so as to have  $U^T m_\nu U = \text{diag}(m_1, m_2, m_3)$ . The light neutrino mass eigenvalues  $m_i$  are given by  $m_i = (y v_u)^2 / M_{Ri}$ , and they can be made real and positive since the phase of  $y$  can be absorbed due to redefinition of phases in lepton doublets and the phases  $\phi_i$  can be included in the diagonal phase matrix of  $U$ . As previously discussed, this structure of  $M_R$  is not useful in explaining the nonzero  $\theta_{13}$ , as seen while comparing the above form of  $U$  and  $U_{PMNS}$ . Since the measured value of  $\theta_{13}$  is not very small, it is difficult to reconcile  $\theta_{13}$  just by deforming  $m_\nu$  from its above form with the introduction of small expansion parameter [33]. Rather we should have deformation parameter at the same order of the existing elements in  $m_\nu$ . In our framework, we have introduced the  $\xi'$  field for this purpose.

### 3.1 RH Neutrinos

The new scalar singlet  $\xi'$  contributes to the heavy RH neutrino sector through the  $x_N \xi' (N^c N^c)$  term and the Majorana neutrino mass matrix then takes the form of  $M_{Rd}$  as in Eq.(2.6). We note that after having a rotation by  $U_{TB}$ , the  $M_{Rd}$  takes the form as given by,

$$U_{TB}^T M_{Rd} U_{TB} = \begin{bmatrix} a + b - \frac{d}{2} & 0 & -\frac{\sqrt{3}}{2}d \\ 0 & a + d & 0 \\ -\frac{\sqrt{3}}{2}d & 0 & -a + b + \frac{d}{2} \end{bmatrix}. \quad (3.2)$$

Therefore a further rotation by  $U_1$  (another unitary matrix) takes the matrix  $M_{Rd}$  to a diagonal one,  $\text{diag}(M_1 e^{i\varphi_1}, M_2 e^{i\varphi_2}, M_3 e^{i\varphi_3}) = (U_{TB} U_1)^T M_{Rd} U_{TB} U_1$ , where  $M_{i=1,2,3}$  are given by,

$$M_1 = |b + \sqrt{a^2 + d^2 - ad}| = |a| \left| \lambda_2 e^{i\phi_{ba}} + \sqrt{1 + \lambda_1^2 e^{2i\phi_{da}} - \lambda_1 e^{i\phi_{da}}} \right|, \quad (3.3)$$

$$M_2 = |a + d| = |a| \left| 1 + \lambda_1 e^{i\phi_{da}} \right|, \quad (3.4)$$

$$M_3 = |b - \sqrt{a^2 + d^2 - ad}| = |a| \left| \lambda_2 e^{i\phi_{ba}} - \sqrt{1 + \lambda_1^2 e^{2i\phi_{da}} - \lambda_1 e^{i\phi_{da}}} \right|, \quad (3.5)$$

with  $\lambda_1 = |d/a|$  and  $\lambda_2 = |b/a|$ .  $\phi_{da} = \phi_d - \phi_a$  and  $\phi_{ba} = \phi_b - \phi_a$  are the phase differences between  $(d, a)$  and  $(b, a)$  respectively. Phases associated with the above masses can be written as

$$\varphi_1 = \arg(b + \sqrt{a^2 + d^2 - ad}), \quad (3.6)$$

$$\varphi_2 = \arg(a + d), \quad (3.7)$$

$$\varphi_3 = \arg(b - \sqrt{a^2 + d^2 - ad}). \quad (3.8)$$

For simplicity, we will work with  $\phi_{da} = 0$ . Hence above set of eigenvalues and phases can be rewritten as

$$M_1 = |a| \left| \lambda_2 e^{i\phi_{ba}} + K \right| \quad \varphi_1 = \arg(b + aK), \quad (3.9)$$

$$M_2 = |a| |1 + \lambda_1| \quad \varphi_2 = \arg(a + d), \quad (3.10)$$

$$M_3 = |a| \left| \lambda_2 e^{i\phi_{ba}} - K \right| \quad \varphi_3 = \arg(b - aK), \quad (3.11)$$

where  $K = \sqrt{1 - \lambda_1 + \lambda_1^2}$ .

### 3.2 Light Neutrino Masses and Mixing Angles

Light neutrino masses obtained via type-I see-saw mechanism through  $m_\nu = m_D^T M_{Rd}^{-1} m_D$  is now given by  $m_D^T U_R U_m^* [\text{diag}(M_1, M_2, M_3)]^{-1} U_m^* U_R^T m_D$  where  $U_R = U_{TB} U_1$  and  $U_m = \text{diag}(e^{i\varphi_1/2}, e^{i\varphi_2/2}, e^{i\varphi_3/2})$ . The special form of  $m_D$  (see in Eq.(2.4)) suggests that  $U_R$ , with the second and third rows interchanged, will be the diagonalizing matrix of the light neutrino mass matrix  $m_\nu$  apart from the diagonal phase matrix. Since the charged lepton mass matrix is already diagonal, the lepton mixing matrix is given by [20]

$$U_\nu = \frac{m_D^T}{y v_u} U_{TB} U_1^* \text{diag}(e^{i\varphi_1/2}, e^{i\varphi_2/2}, e^{i\varphi_3/2}), \quad (3.12)$$

so that  $m_\nu = U_\nu^* \text{diag}(m_i) U_\nu^\dagger$ . Note that, the light neutrino masses  $m_{1,2,3}$  (real and positive) are given by

$$m_i = \frac{(y v_u)^2}{M_i}, \quad (3.13)$$

where  $M_{i=1,2,3}$  are taken from Eq.(3.9 - 3.11). We can now remove one common phase by setting  $\varphi_1 = 0$ . Hence, the final form of unitary matrix that diagonalizes  $m_\nu$  is given by

$$\begin{aligned} U_\nu &= \frac{m_D^T}{y v_u} U_{TB} \begin{bmatrix} \cos \theta & 0 & \sin \theta e^{-i\psi} \\ 0 & 1 & 0 \\ -\sin \theta e^{i\psi} & 0 & \cos \theta \end{bmatrix} \text{diag}(1, e^{i\varphi_2/2}, e^{i\varphi_3/2}), \quad (3.14) \\ &= \begin{bmatrix} \sqrt{\frac{2}{3}} \cos \theta & 1/\sqrt{3} & \sqrt{\frac{2}{3}} \sin \theta e^{-i\psi} \\ -\frac{\cos \theta}{\sqrt{6}} + \frac{\sin \theta}{\sqrt{2}} e^{i\psi} & 1/\sqrt{3} & -\frac{\cos \theta}{\sqrt{2}} - \frac{\sin \theta}{\sqrt{6}} e^{-i\psi} \\ -\frac{\cos \theta}{\sqrt{6}} - \frac{\sin \theta}{\sqrt{2}} e^{i\psi} & 1/\sqrt{3} & \frac{\cos \theta}{\sqrt{2}} - \frac{\sin \theta}{\sqrt{6}} e^{-i\psi} \end{bmatrix} \cdot \begin{bmatrix} 1 & 0 & 0 \\ 0 & e^{i\varphi_2/2} & 0 \\ 0 & 0 & e^{i\varphi_3/2} \end{bmatrix}, \quad (3.15) \end{aligned}$$

where we have parametrized the extra  $U_1$  matrix by  $\theta$  and  $\psi$  and employed Eqs.(2.4) and (3.1). We identify the Majorana phases as

$$\varphi_2 = \alpha_{21} \quad \text{and} \quad \varphi_3 = \alpha_{31}. \quad (3.16)$$

In this type of model, using Eqs.(3.9 - 3.11) and Eq.(3.13) we find a general sum rule for light neutrino masses satisfying

$$\frac{1}{m_1} - \frac{2Ke^{i\alpha_{21}}}{m_2(1 + \lambda_1)} = \frac{e^{i\alpha_{31}}}{m_3}. \quad (3.17)$$

Note that in the limit  $K \rightarrow 1$  (*i.e.* with  $\lambda_1 = 0$ ), the sum rule is reduced to the one found in [27, 34]. The Majorana phases  $\alpha_{21}$  and  $\alpha_{31}$  are therefore related to the light neutrino masses. They will play important role in leptogenesis, which we discuss in section 5. The sum rule may carry important consequence in neutrinoless double beta decay. A study with different sum rules in this direction can be found in [35].

The charged lepton mass-matrix being diagonal, the above form of  $U_\nu$  leads to (see Eq.1.2)

$$\sin \theta_{13} = \sqrt{\frac{2}{3}} \sin \theta, \quad \delta = \psi; \quad (3.18)$$

$$\sin^2 \theta_{12} = \frac{1}{3(1 - \sin^2 \theta_{13})} \quad \text{and} \quad \sin^2 \theta_{23} = \frac{1}{2} + \frac{1}{\sqrt{2}} \sin \theta_{13} \cos \delta, \quad (3.19)$$

up to the order  $\sin^2 \theta_{13}$ . The study of these correlations in presence of  $A_4$  are available in the literature [20, 22, 36]. For rest of our analysis we will consider  $\psi = 0$ . The mixing angle  $\theta$  is then given by

$$\tan 2\theta = \frac{\sqrt{3}\lambda_1}{(2 - \lambda_1)}. \quad (3.20)$$

We have studied the variation of  $\sin^2 \theta_{13}$  against the parameter  $\lambda_1$  in Fig.1, where the  $1\sigma$

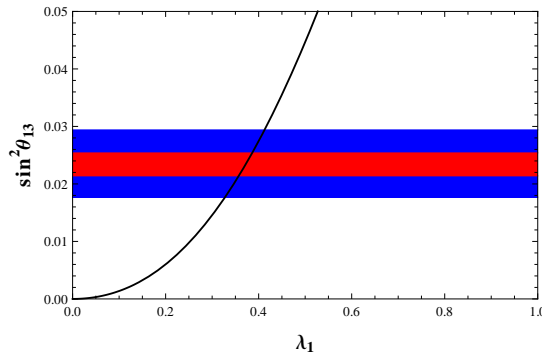


Figure 1:  $\sin^2 \theta_{13}$  vs  $\lambda_1$  (*i.e.*  $|d/a|$ ) plot. Horizontal blue shaded region stands for  $3\sigma$  allowed range for  $\sin^2 \theta_{13}$  and the red shaded region inside represents  $1\sigma$  range for  $\sin^2 \theta_{13}$  obtained from [8].

and  $3\sigma$  allowed regions for  $\sin^2 \theta_{13}$  obtained from [8] are also indicated in the same by red

and blue horizontal shaded regions respectively for both NH and IH. We observe that for NH, best fit [8] value of  $\sin^2 \theta_{13}$  ( $=0.0234$ ) corresponds to  $\lambda_1 = 0.37$  and that one for IH ( $\sin^2 \theta_{13} = 0.024$ ) corresponds to  $\lambda_1 = 0.38$ . We also note that the  $3\sigma$  range of  $\sin^2 \theta_{13}$  covers a narrow interval of  $\lambda_1$  that can be approximately expressed as  $0.33 \lesssim \lambda_1 \lesssim 0.41$  as seen from Fig.1 for both NH and IH.

The other mixing angles  $\theta_{12}$  and  $\theta_{23}$  are also studied through the variation of  $\sin^2 \theta_{12}$  and  $\sin^2 \theta_{23}$  against  $\lambda_1$ , using Eq.(3.19) in Fig.2. Note that once we restrict  $\lambda_1$  to be in the above mentioned range (indicated in Fig.2 by vertical (blue) patches) so that  $\sin^2 \theta_{13}$  falls within the  $3\sigma$  allowed range, it constraints the ranges of  $\sin^2 \theta_{12}$  and  $\sin^2 \theta_{23}$  in our set-up. This result is mentioned in Table 3 as obtained from Fig.2. The ranges are well within the  $3\sigma$  allowed regions of  $\sin^2 \theta_{12}$  and  $\sin^2 \theta_{23}$  [8]. So we conclude that this particular range of  $\lambda_1$  ( $0.33 \lesssim \lambda_1 \lesssim 0.41$ ) is consistent in producing all the three mixing angles successfully, and we will use this range of  $\lambda_1$ , while studying any other observables against  $\lambda_1$  unless otherwise stated.

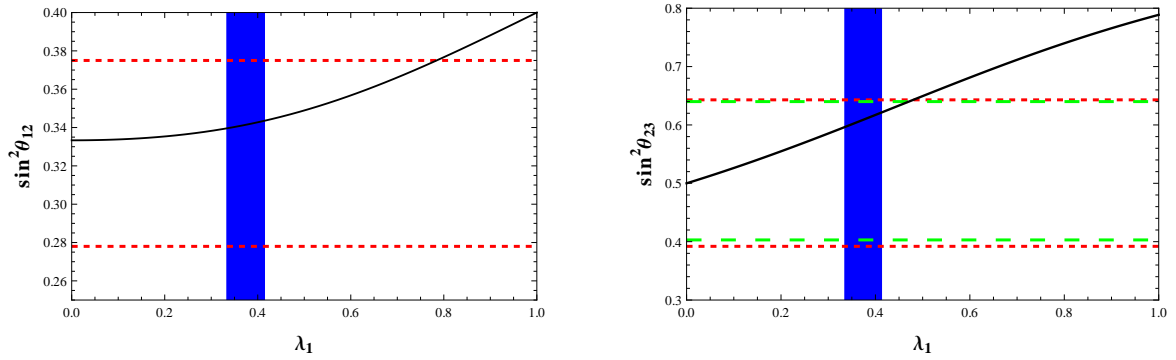


Figure 2:  $\lambda_1$  dependence of  $\sin^2 \theta_{12}$  and  $\sin^2 \theta_{23}$ . Vertical blue patch indicates the restricted region of parameter space for  $\lambda_1$  obtained from Fig.1. Horizontal red dashed lines represent  $3\sigma$  allowed range for  $\sin^2 \theta_{12}$  in the left panel, while in the right panel horizontal red dashed and green large-dashed lines represent  $3\sigma$  allowed regions for  $\sin^2 \theta_{23}$  both NH and IH respectively as in [8].

Range of $\lambda_1$ obtained from Fig.1	$\sin^2 \theta_{12}$	$\sin^2 \theta_{23}$
$0.36 \lesssim \lambda_1 \lesssim 0.39$	0.341-0.342	0.604-0.614
$0.33 \lesssim \lambda_1 \lesssim 0.41$	0.339-0.343	0.595-0.620

Table 3: Allowed regions of  $\sin^2 \theta_{12}$  and  $\sin^2 \theta_{23}$  obtained from Fig.2 for a restricted range of  $\lambda_1$  (corresponding to Fig.1) in our set-up.

## 4 Constraints on parameters from neutrino oscillation data

Apart from  $\lambda_1$ , we have other parameters  $\lambda_2$ ,  $|a|$  and  $\phi_{ba}$  (after setting  $\phi_{da} = 0$ ) in the right handed neutrino sector. Note that  $\lambda_1$ ,  $\lambda_2$  and  $\phi_{ba}$  can be constrained by neutrino oscillation data through the ratio of solar and atmospheric mass-squared differences ( $\Delta m_\odot^2$  and  $|\Delta m_A^2|$  respectively) defined by  $r = \frac{\Delta m_\odot^2}{|\Delta m_A^2|}$  as exercised in [27, 34]. These mass-squared differences are defined as  $\Delta m_\odot^2 = \Delta m_{21}^2 = m_2^2 - m_1^2$  and  $|\Delta m_A^2| = |\Delta m_{31}^2| = m_3^2 - m_1^2 \approx |\Delta m_{32}^2| = m_3^2 - m_2^2$ . Following [8], the best fit values of  $\Delta m_\odot^2 = 7.60 \times 10^{-5} \text{ eV}^2$  (for both NH and IH) and  $|\Delta m_A^2| = 2.48 \times 10^{-3} \text{ eV}^2$  [NH] (and  $|\Delta m_A^2| = 2.38 \times 10^{-3} \text{ eV}^2$  [IH]) will be used in our analysis. Using Eqs.(3.9 - 3.11 and 3.13) we obtain  $r$  in terms of parameters involved in our framework as given by

$$r = \frac{[\lambda_2^2 + 2\lambda_2 K \cos \phi_{ba} + K^2 - (1 + \lambda_1)^2](\lambda_2^2 - 2\lambda_2 K \cos \phi_{ba} + K^2)}{4(1 + \lambda_1)^2 \lambda_2 K |\cos \phi_{ba}|}. \quad (4.1)$$

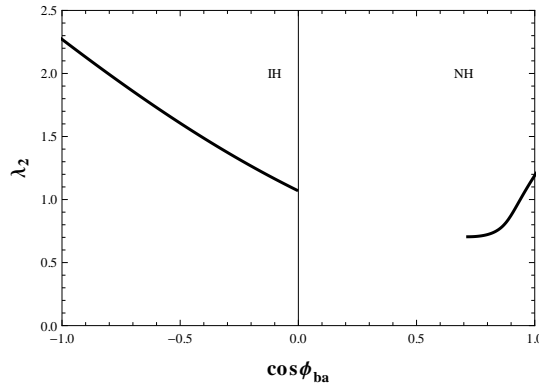


Figure 3: Variation of  $\lambda_2$  with  $\cos \phi_{ba}$ . Here we have fixed  $\lambda_1=0.37$  for NH and  $\lambda_1=0.38$  for IH.

We recall that  $\phi_{ba}$  is the relative phase between parameters  $b$  and  $a$ . Note that with  $\lambda_1 = 0$ ,  $K$  becomes unity and the expression for  $r$  gets back the form in [34]. Considering  $\lambda_1 < 1$  (as required for  $\theta_{13}$  being in the acceptable range, see Fig.1) and as  $\phi_{da} = 0$ ,  $K$  becomes real and considered to be positive. Then as is evident from Eq.(3.9 - 3.11) and Eq.(3.13),  $\cos \phi_{ba} > 0$  for NH and  $\cos \phi_{ba} < 0$  for IH. Using  $r = 0.03$  [8], we can use Eq.(4.1) now to study the correlation between  $\lambda_2$  and  $\cos \phi_{ba}$  as shown in Fig.3. In doing so, we have set the value of  $\lambda_1$  to be 0.37 (0.38) which corresponds to the best fit value of  $\sin^2 \theta_{13}$  for NH (IH) as stated before. Obviously the right panel of the plot corresponds to NH (as  $\cos \phi_{ba} > 0$ ) and left panel is for IH (as  $\cos \phi_{ba} < 0$ ). We find that for NH, with  $\lambda_1 = 0.37$ ,  $\lambda_2$  is restricted to be in the range 0.71 – 1.2 and for IH, with  $\lambda_1 = 0.38$ ,  $\lambda_2$  falls within<sup>1</sup> the range 1.1 – 2.3. It will

<sup>1</sup>Eq.(4.1) describes a quadratic equation of  $|\cos \phi_{ba}|$  once other parameters are fixed. The range of  $\lambda_2$  between 0 and 0.71 is excluded to keep the discriminant positive for  $\lambda_1=0.37$  (for NH).

be further modified as we proceed after including the constraint on the sum of all the light neutrinos from the Planck data [37].

The light neutrino mass  $m_1$  in this framework can be expressed as

$$m_1^2 = |\Delta m_A^2| r \frac{(1 + \lambda_1)^2}{[\lambda_2^2 + 2\lambda_2 K \cos \phi_{ba} + K^2 - (1 + \lambda_1)^2]}. \quad (4.2)$$

Now using the best fit value of  $|\Delta m_A^2| = 2.48 \times 10^{-3} \text{eV}^2$  [NH] ( $2.38 \times 10^{-3} \text{eV}^2$  [IH]),  $r = 0.03$  and  $\lambda_1 = 0.37$  (0.38), we can estimate  $m_1$  from the above relation for NH (IH), shown in Fig.4, as a function of  $\lambda_2$ . Similarly  $m_2$  and  $m_3$  are also plotted in Fig.4. Note that in doing

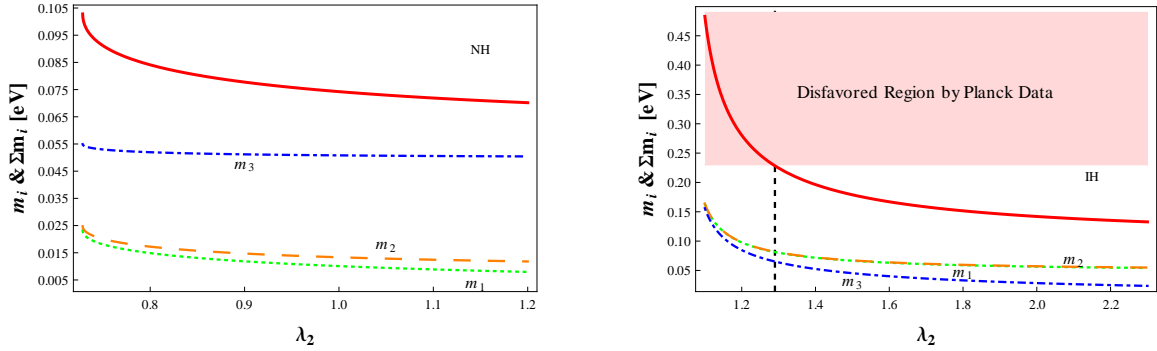


Figure 4: Light neutrino masses  $m_i$ 's and their sum,  $\sum m_i$ , as a function of  $\lambda_2$  for NH ( $\lambda_1 = 0.37$ ) and IH ( $\lambda_1 = 0.38$ ). Here in the right panel the shaded region indicates the disfavored values of  $\sum m_i$ . This makes allowed range for  $\lambda_2$  more restricted for IH, indicated by the vertical black dashed line.

this, the correct sign of  $\cos \phi_{ba}$  in Eq.(4.2) needs to be taken into account while NH and IH cases are considered. The lightest neutrino mass  $m_1$  ( $m_3$ ) falls in the range  $0.008 \text{ eV} \lesssim m_1 \lesssim 0.02 \text{ eV}$  for NH ( $0.02 \text{ eV} \lesssim m_3 \lesssim 0.12 \text{ eV}$  for IH). In this plot we have also shown the sum of the light neutrino masses,  $\sum m_i$ . From Fig.4, we conclude that it lies in the range  $0.07 \text{ eV} \lesssim \sum m_i \lesssim 0.1 \text{ eV}$  for NH and  $0.13 \text{ eV} \lesssim \sum m_i \lesssim 0.28 \text{ eV}$  for IH. The Planck data along with external CMB and BAO results [37] provide an upper bound as  $\sum m_i \lesssim 0.23 \text{ eV}$ . Once this is considered, the range of  $\sum m_i$  as obtained from our analysis for NH would not be affected. However in case of IH, it further restricts the range of  $\lambda_2$  ( $1.3 \lesssim \lambda_2 \lesssim 2.3$ , indicated by vertical dashed line) as observed from the shaded region of Fig.4, right panel. So the model's prediction for sum of all three light neutrino masses turns out to be,

$$0.07 \text{ eV} \lesssim \sum_{i=1}^3 m_i \lesssim 0.1 \text{ eV (NH)} \quad \& \quad 0.13 \text{ eV} \lesssim \sum_{i=1}^3 m_i \lesssim 0.23 \text{ eV (IH)}. \quad (4.3)$$

In our analysis we can comment also on the relative magnitudes of heavy RH neutrinos. For NH we obtain  $M_1 \simeq (1.1 - 1.5)M_2 \simeq (2.7 - 6.6)M_3$  and for IH we have  $M_1 \simeq M_2 \simeq \frac{M_3}{1.2-2.3}$ . So, in the present set-up Majorana neutrinos are not strongly hierarchical.

Two Majorana phases  $\alpha_{21}$  and  $\alpha_{31}$  can be investigated in the set-up in a similar way as done in [27]. Here in the model under consideration, we find Majorana phases  $\alpha_{21}$  and  $\alpha_{31}$  in terms of  $\lambda_1$ ,  $\lambda_2$  and  $\phi_{ba}$  as given by

$$\tan \alpha_{21} = -\frac{\lambda_2 \sin \phi_{ba}}{K + \lambda_2 \cos \phi_{ba}}, \quad (4.4)$$

$$\tan \alpha_{31} = \frac{2K\lambda_2 \sin \phi_{ba}}{\lambda_2^2 - K^2}. \quad (4.5)$$

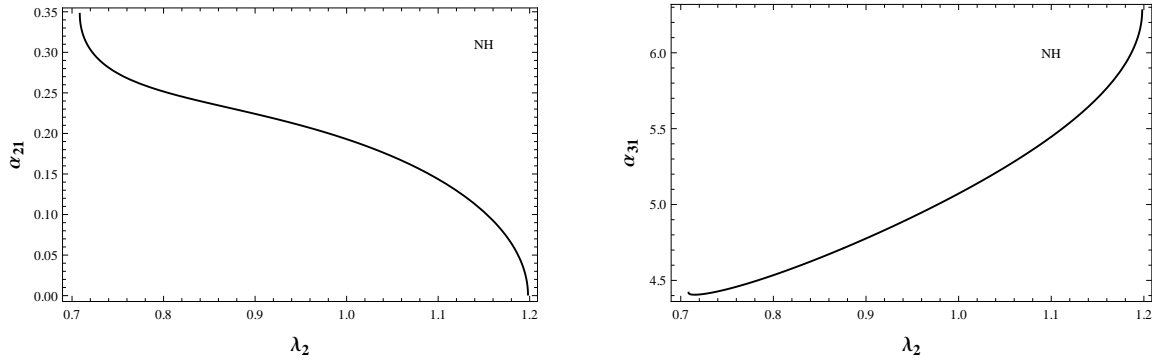


Figure 5: Variation of Majorana phases ( $\alpha_{21}$ : left panel;  $\alpha_{31}$ : right panel) with  $\lambda_2$  for NH.

Note that there exists a relative sign between  $\sin \alpha_{21}$  and  $\sin \alpha_{31}$  as observed from the neutrino mass sum rule in Eq.(3.17). For NH,  $\cos \phi_{ba} > 0$  as discussed before and  $\sin \phi_{ba} < 0$  is considered in order to produce correct sign of baryon asymmetry [27]. Similarly, for IH we have  $\cos \phi_{ba} < 0$  and  $\sin \phi_{ba} < 0$ . Taking all this into consideration, Eqs.(4.4) and (4.5) can successfully correlate Majorana phases ( $\alpha_{21}$  and  $\alpha_{31}$ ) with parameters  $\lambda_1$  and  $\lambda_2$ . We have plotted variation of  $\alpha_{21}$  and  $\alpha_{31}$  with  $\lambda_2$  for both NH and IH in Fig.5 and Fig.6 respectively. As before we have fixed  $\lambda_1 = 0.37$  for NH ( $\lambda_1 = 0.38$  for IH). This study of Majorana phases

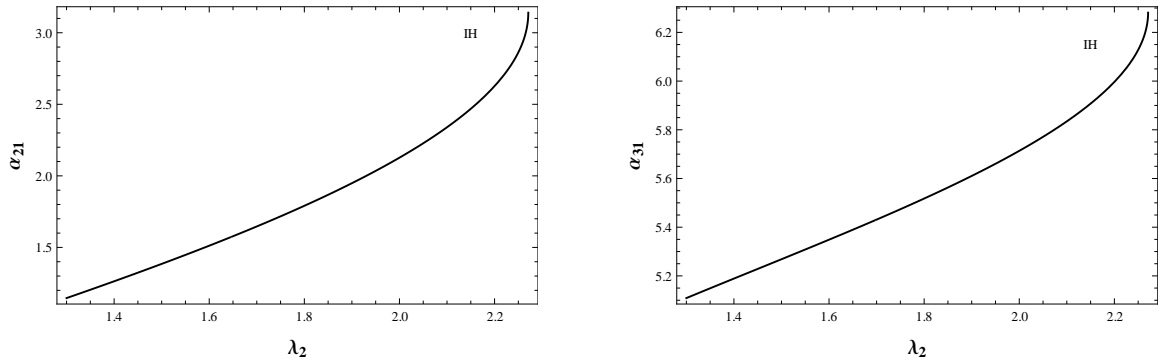


Figure 6: Variation of Majorana phases ( $\alpha_{21}$ : left panel;  $\alpha_{31}$ : right panel) with  $\lambda_2$  for IH.

will be particularly useful when we will study the dependence of CP-violating parameter

$\epsilon_i$  in our model on  $\lambda_2$ . Effective neutrino mass parameter,  $|\langle m \rangle|$ , is an important quantity which controls the neutrinoless double beta decay. In our model, the effective neutrino mass parameter is obtained as [5, 38]

$$|\langle m \rangle| = \left| \frac{2}{3}m_1 \cos^2 \theta + \frac{1}{3}m_2 e^{i\alpha_{21}} + \frac{2}{3}m_3 \sin^2 \theta e^{i\alpha_{31}} \right|. \quad (4.6)$$

Since the dependence of  $m_i$  and  $\alpha_{21,31}$  on  $\lambda_2$  (for fixed  $\lambda_1$ ) is known (from Fig.4, 5 and 6), we plot  $|\langle m \rangle|$  as a function of  $\lambda_2$  with  $\lambda_1 = 0.37$  for NH and  $\lambda_1 = 0.38$  for IH in Fig.7. We found

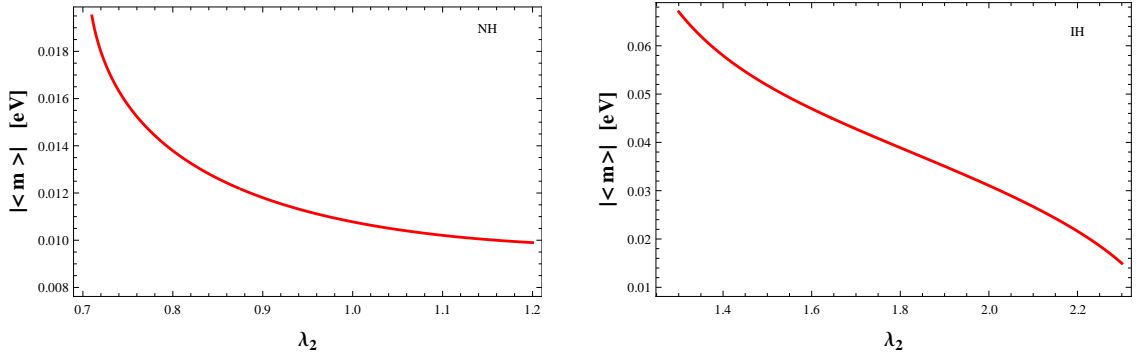


Figure 7: Variation of  $|\langle m \rangle|$  with  $\lambda_2$  for NH (left panel) and IH (right panel) respectively.

the range for the  $|\langle m \rangle|$  as  $0.01 \text{ eV} < |\langle m \rangle| < 0.02 \text{ eV}$  for NH and  $0.015 \text{ eV} < |\langle m \rangle| < 0.067 \text{ eV}$  for IH. The current upper limit on  $|\langle m \rangle|$  however varies between 0.177 eV and 0.339 eV taking into account the different choices of nuclear matrix elements [39].

## 5 Leptogenesis

The presence of see-saw realization of light neutrino mass in the model under consideration gives the opportunity to study leptogenesis as the heavy RH neutrinos are already present in the model. It allows the generation of lepton asymmetry through the out-of-equilibrium decay of heavy RH neutrinos in the early Universe. This lepton asymmetry can be converted into baryon asymmetry of the Universe with the help of sphaleron process. With the consideration that the generation of lepton asymmetry happens at a temperature of the Universe  $T \sim M_i \gtrsim (1 + \tan^2 \beta) 10^{12} \text{ GeV}$  (where  $\tan \beta = v_u/v_d$ ), it does not distinguish between flavors, the so called ‘one-flavor approximation’ regime [27–30] is achieved. The CP-asymmetry generated by the out-of-equilibrium decay of each RH neutrinos (and sneutrinos) is given by [?, 40–45]

$$\epsilon_i = \frac{1}{8\pi} \sum_{j \neq i} \frac{\text{Im} \left[ \left( (\hat{Y}_\nu \hat{Y}_\nu^\dagger)_{ji} \right)^2 \right]}{(\hat{Y}_\nu \hat{Y}_\nu^\dagger)_{ii}} f \left( \frac{m_i}{m_j} \right), \quad (5.1)$$



where  $\hat{Y}_\nu$  is the effective Yukawa coupling matrix for neutrinos in the basis where RH neutrino mass matrix  $M_{Rd}$  is diagonal <sup>2</sup>. In the present set-up,  $\hat{Y}_\nu = \text{diag}(1, e^{-i\alpha_{21}/2}, e^{-i\alpha_{31}/2}) U_R^T Y_\nu$ , where  $U_R = U_{TB} U_1$ . The loop factor  $f(x)$  in the above expression (the model being supersymmetric) is defined as follows [46]

$$f(x) \equiv -x \left[ \frac{2}{x^2 - 1} + \ln \left( 1 + \frac{1}{x^2} \right) \right], \quad (5.2)$$

with  $x = m_i/m_j$ . The total lepton asymmetry receives contribution from the decay of all three RH neutrinos (and sneutrinos).

It has been observed that at LO, (*i.e.* when  $Y_\nu = Y_{\nu 0}$ ) product of the effective Yukawa coupling matrices  $\hat{Y}_{\nu 0} \hat{Y}_{\nu 0}^\dagger$  is proportional to a unit matrix, hence lepton asymmetry parameter  $\epsilon_i$  vanishes [25]. However considering NLO corrections to the Yukawa, we have obtained Eq.(2.7). Therefore using Eq.(2.7),  $\hat{Y}_\nu \hat{Y}_\nu^\dagger$  becomes

$$\begin{aligned} \hat{Y}_\nu \hat{Y}_\nu^\dagger = y^2 \mathbf{I} + & \begin{bmatrix} \cos 2\theta & \sqrt{2} e^{\frac{i\alpha_{21}}{2}} \cos \theta & e^{\frac{i\alpha_{31}}{2}} \sin 2\theta \\ \sqrt{2} e^{-\frac{i\alpha_{21}}{2}} \cos \theta & 0 & \sqrt{2} e^{\frac{i(\alpha_{31}-\alpha_{21})}{2}} \sin \theta \\ e^{-\frac{i\alpha_{31}}{2}} \sin 2\theta & \sqrt{2} e^{-\frac{i(\alpha_{31}-\alpha_{21})}{2}} \sin \theta & -\cos 2\theta \end{bmatrix} (2\text{Re}(x_C)\kappa y) \\ & + \begin{bmatrix} -\frac{\sin 2\theta}{\sqrt{3}} & \sqrt{\frac{2}{3}} e^{\frac{i\alpha_{21}}{2}} \sin \theta & \frac{1}{\sqrt{3}} e^{\frac{i\alpha_{31}}{2}} \cos 2\theta \\ \sqrt{\frac{2}{3}} e^{-\frac{i\alpha_{21}}{2}} \sin \theta & 0 & -\sqrt{\frac{2}{3}} e^{\frac{i(\alpha_{31}-\alpha_{21})}{2}} \cos \theta \\ \frac{1}{\sqrt{3}} e^{-\frac{i\alpha_{31}}{2}} \cos 2\theta & -\sqrt{\frac{2}{3}} e^{-\frac{i(\alpha_{31}-\alpha_{21})}{2}} \cos \theta & \frac{1}{\sqrt{3}} \sin 2\theta \end{bmatrix} (2\text{Re}(x_D)\kappa y). \end{aligned} \quad (5.3)$$

Note that having origin related to a NLO correction term,  $\kappa$  in general is expected to be small,  $\kappa = v_T/\Lambda \ll 1$ . Hence the expression of Eq. (5.3) is kept up to first order in  $\kappa$ . Finally in our framework the CP-asymmetry parameters corresponding to all three RH neutrinos,  $\epsilon_{1,2,3}$  take the form as

$$\begin{aligned} \epsilon_1 = \frac{-\kappa^2}{2\pi} & \left[ \sin \alpha_{21} \left( 2\text{Re}(x_C)^2 \cos^2 \theta + \frac{2\text{Re}(x_D)^2}{3} \sin^2 \theta + \frac{2\text{Re}(x_C)\text{Re}(x_D)}{\sqrt{3}} \sin 2\theta \right) f\left(\frac{m_1}{m_2}\right) \right. \\ & \left. + \sin \alpha_{31} \left( \text{Re}(x_C)^2 \sin^2 2\theta + \frac{\text{Re}(x_D)^2}{3} \cos^2 2\theta + \frac{\text{Re}(x_C)\text{Re}(x_D)}{\sqrt{3}} \sin 4\theta \right) f\left(\frac{m_1}{m_3}\right) \right], \end{aligned} \quad (5.4)$$

$$\begin{aligned} \epsilon_2 = \frac{\kappa^2}{2\pi} & \left[ \sin \alpha_{21} \left( 2\text{Re}(x_C)^2 \cos^2 \theta + \frac{2\text{Re}(x_D)^2}{3} \sin^2 \theta + \frac{2\text{Re}(x_C)\text{Re}(x_D)}{\sqrt{3}} \sin 2\theta \right) f\left(\frac{m_2}{m_1}\right) \right. \\ & \left. - \sin(\alpha_{31} - \alpha_{21}) \left( 2\text{Re}(x_C)^2 \sin^2 \theta + \frac{2\text{Re}(x_D)^2}{3} \cos^2 \theta - \frac{2\text{Re}(x_C)\text{Re}(x_D)}{\sqrt{3}} \sin 2\theta \right) f\left(\frac{m_2}{m_3}\right) \right], \end{aligned} \quad (5.5)$$

$$\begin{aligned} \epsilon_3 = \frac{\kappa^2}{2\pi} & \left[ \sin \alpha_{31} \left( \text{Re}(x_C)^2 \sin^2 2\theta + \frac{\text{Re}(x_D)^2}{3} \cos^2 2\theta + \frac{\text{Re}(x_C)\text{Re}(x_D)}{\sqrt{3}} \sin 4\theta \right) f\left(\frac{m_3}{m_1}\right) \right. \\ & \left. + \sin(\alpha_{31} - \alpha_{21}) \left( 2\text{Re}(x_C)^2 \sin^2 \theta + \frac{2\text{Re}(x_D)^2}{3} \cos^2 \theta - \frac{2\text{Re}(x_C)\text{Re}(x_D)}{\sqrt{3}} \sin 2\theta \right) f\left(\frac{m_3}{m_2}\right) \right]. \end{aligned} \quad (5.6)$$

---

<sup>2</sup>Here Eq.(3.13) is used to express the loop factor  $f$  in terms of the ratio of light neutrino masses.

Lepton asymmetry in this scenario therefore depends on light neutrino masses  $m_i$  (through loop factor), Majorana phases  $\alpha_{21,31}$ , couplings  $\text{Re}(x_{C,D})$ ,  $\kappa$  (coming from the NLO correction terms in Yukawa) and interestingly on  $\theta$  (and hence on  $\lambda_1$ ). Recall that  $\theta$  was originated from the deviation from the exact tri-bimaximal mixing and therefore leads to nonzero  $\sin \theta_{13}$ . We will come back to discuss it, before that let us discuss how this lepton asymmetry parameter is connected with observed baryon asymmetry of the Universe.

Lepton asymmetry can be linked to the baryon asymmetry [24, 47–49] as

$$Y_B = -1.48 \times 10^{-3} \sum_i \epsilon_i \eta_{ii}. \quad (5.7)$$

Here  $\eta_{ii}$  stands for the efficiency factor [46]. We consider the efficiency factor to be given by

$$\frac{1}{\eta_{ii}} \approx \frac{3.3 \times 10^{-3} \text{ eV}}{\tilde{m}_i} + \left( \frac{\tilde{m}_i}{0.55 \times 10^{-3} \text{ eV}} \right)^{1.16}, \quad (5.8)$$

with  $\tilde{m}_i$  as the washout mass parameter,  $\tilde{m}_i = \frac{(\hat{Y}_\nu \hat{Y}_\nu^\dagger)_{ii} v_u^2}{M_i} \simeq m_i$  to the leading order. The above expression is valid for  $M_i < 10^{14} \text{ GeV}$  [50]. This upper bound on  $M_i$  is also consistent in keeping the lepton number violating decays within the experimental limit [50, 51]. As we already have a lower bound on  $M_i$  from the ‘one-flavor approximation’, it turns out that low values of  $\tan \beta$  are favored for this scenario to work<sup>3</sup>. Interestingly in [52], the authors have shown that if the scale of supersymmetry breaking ( $m_s$ ) in MSSM is sufficiently large (say  $\sim 10 \text{ TeV}$  or so) the low  $\tan \beta$  region  $\tan \beta \lesssim (3 - 5)$  is consistent with the results of LHC so far. Such large value of  $m_s$  on the other hand can in principle reduce the branching ratio for the LFV processes. However the details of this conjecture is beyond the scope of the present study.

### 5.1 Leptogenesis with fixed $\lambda_1$ and varying $\lambda_2$

In this section we will study the range of the parameters involved in  $Y_B$  expression so as to reproduce the correct amount of matter-antimatter asymmetry of the Universe. The observed value of  $Y_B$  is reported to be [53]

$$Y_B = (8.79 \pm 0.20) \times 10^{-11}. \quad (5.9)$$

As the efficiency factor ( $\eta_{ii}$ ) is found to be  $\sim \mathcal{O}(10^{-2})$ ,  $\epsilon_i$  should be of order  $\mathcal{O}(10^{-6})$  in order to reproduce the correct amount of baryon asymmetry of the Universe. As discussed earlier, we have kept  $\lambda_1$  to be fixed at 0.37 for NH (0.38 for IH) which correspond to the best fit value of  $\sin^2 \theta_{13}$  [8]. We further note that the expression of  $Y_B$  involves  $\theta$  which in turn is related

---

<sup>3</sup> $y$  is expected to be  $\sim \mathcal{O}(10^{-1})$  in order to reproduce correct  $m_i$  for this range of  $M_i$ .

to  $\theta_{13}$ . So once  $\lambda_1$  is fixed it would correspond to a particular value of  $\theta$ . The expansion parameter  $\kappa = v_T/\Lambda$  is taken to be  $\sim 10^{-2}$ . The variation of  $\alpha_{21,31}$  and  $m_i$ 's with  $\lambda_2$  (for  $\lambda_1 = 0.37, 0.38$  for NH and IH respectively) are already studied. Using those information, we can study the dependence of  $Y_B$  on  $\lambda_2$  for fixed values of  $\text{Re}(x_C)$  and  $\text{Re}(x_D)$ . The first bracketed expression in Eqs.(5.4 - 5.6) therefore serves merely as constant factor.

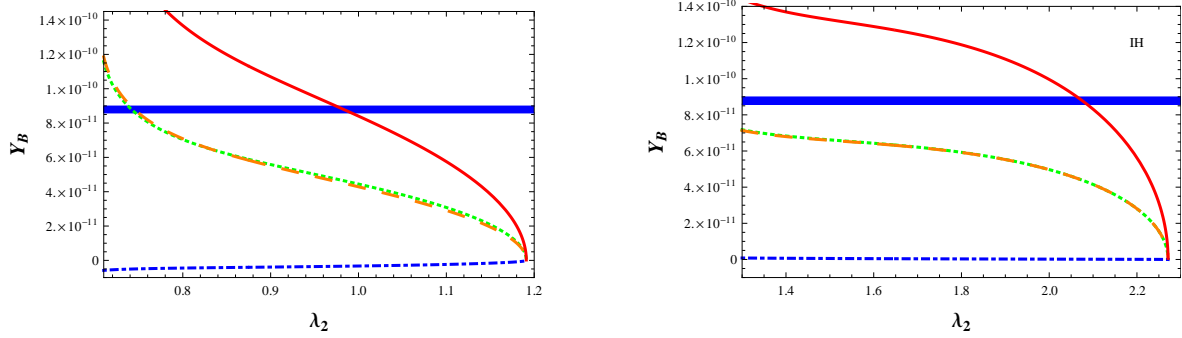


Figure 8: Baryon asymmetry of the Universe as function of  $\lambda_2$  for NH (with  $\lambda_1 = 0.37$ , left panel) and IH (with  $\lambda_1 = 0.38$ , right panel). Here, red continuous line, orange large dashed line, green dotted line and blue dot-dashed line stand for total  $Y_B$ ,  $Y_{B1,2,3}$  respectively. The horizontal blue patch represents allowed range for total baryon asymmetry. For NH we have taken  $\text{Re}(x_C) = \text{Re}(x_D) = 0.2$  and for IH we have  $\text{Re}(x_C) = \text{Re}(x_D) = 0.05$ . For both cases we have fixed  $\kappa$  at 0.01.

In Fig.8 (left panel), we have plotted total baryon asymmetry  $Y_B$  (red continuous line) along with individual  $Y_{B1,2,3}$  (orange large dashed, green dotted and blue dot-dashed lines respectively) against  $\lambda_2$  for  $\text{Re}(x_C) = \text{Re}(x_D) = 0.2$  in case of NH. Note that the range of  $\lambda_2$  0.71 – 1.2 for NH and 1.3 – 2.3 for IH was already fixed (from Fig. 3 and 4) for  $\lambda_1 = 0.37$  (for NH) and  $\lambda_1 = 0.38$  (for IH) respectively. The relative sign between  $\sin \alpha_{21}$  and  $\sin \alpha_{31}$  is fixed from the sum rule, Eq.(3.17). Their dependence on  $\lambda_2$  is depicted in Fig.5. In producing these plots, we recall that  $\cos \phi_{ba} > 0$  for NH and  $\cos \phi_{ba} < 0$  for IH. Also  $\sin \phi_{ba} < 0$  is considered to produce correct sign of  $Y_B$ . In  $\epsilon_1$ ,  $f(m_1/m_2)$  is of positive sign and remains dominant over  $|f(m_1/m_3)|$  throughout the range of  $\lambda_2$  by orders of magnitude. So an overall negative sign for  $\epsilon_1$  results when combined with  $\sin \alpha_{21} > 0$  and  $\sin \alpha_{31} < 0$  for the range of  $\lambda_2$  inferred from Fig.8. Similar conclusion can be drawn for  $\epsilon_2$ . In this case  $f(m_2/m_1)$  is negative and its magnitude is sufficiently large compared to  $|f(m_2/m_3)|$  so that differences between magnitude of  $\sin \alpha_{21}$  and  $\sin(\alpha_{31} - \alpha_{21})$  can not produce any sizable effect between the two terms (one is the set of terms proportional to  $\sin \alpha_{21}$  and other is the similar set proportional to  $\sin(\alpha_{31} - \alpha_{21})$ ) involved. So  $\epsilon_2$  is effectively dominated by the first term and overall it gives negative contribution. In  $\epsilon_3$ , however both the terms involved contribute almost equally and overall  $\epsilon_3$  contributes with opposite sign (also seen in the Fig.8 terms of  $Y_{B3}$  which is negative, left panel) compared to  $\epsilon_{1,2}$ . As shown in Fig.8 (left panel), contribution from

$Y_{B3}$  is suppressed (and of opposite sign). This is due to the fact that the corresponding washout is larger though in magnitude  $|\epsilon_3| \lesssim |\epsilon_{1,2}|$ . A horizontal patch in Fig.8 is provided to indicate the allowed  $Y_B$  range [53]. It shows that for this specific choice of  $\text{Re}(x_{C,D})=0.2$ , correct amount of baryon asymmetry can be generated in our framework for  $\lambda_2 \sim \mathcal{O}(1)$ . Note that we can achieve this  $Y_B$  for not so large value of  $\text{Re}(x_{C,D})$  in comparison to the findings of [27]. To check the possible values of  $\text{Re}(x_C)$  and/or  $\text{Re}(x_D)$  we have drawn a contour plot in Fig.9 (left panel) between  $\text{Re}(x_D)$  and  $\lambda_2$ , while  $\text{Re}(x_C)=\text{Re}(x_D)$  is assumed as an example. The pattern of  $Y_B$  plot is also different from what was obtained in [27]. This is due to the involvement of nonzero  $\theta$ .

In Fig.8 (right panel), we then plot  $Y_B$ ,  $Y_{B1,2,3}$  vs.  $\lambda_2$  in case of IH with  $\text{Re}(x_C) = \text{Re}(x_D) = 0.05$ . As it was found in section 4,  $\lambda_2$  ranges between 1.3 and 2.3 and  $\cos \phi_{ba} < 0$  and  $\sin \phi_{ba} < 0$  in this case. The Majorana CP-violating phases  $\alpha_{21}$  and  $\alpha_{31}$  are obtained in section 4 as function of  $\lambda_2$  (see Fig.6, with  $\lambda_1 = 0.38$ ). Here  $m_1$  and  $m_2$  are much closer to each other leading to large enhancement in the magnitude of loop factors  $f(m_1/m_2)$  and  $f(m_2/m_1)$ . Their magnitudes are even larger than their counterpart in NH. Variation of these loop factors with  $\lambda_2$  shows that  $f(m_1/m_2) \simeq -f(m_2/m_1) \gg f(m_3/m_{1,2})$  and  $f(m_1/m_2) \simeq -f(m_2/m_1) \gg -f(m_{2,1}/m_3)$ . Overall nonzero CP-violating phases  $\alpha_{21}$  and  $\alpha_{31}$  are required to have leptogenesis but it appears that the final asymmetry is dominated by the loop factors. Though  $Y_{B1}$  and  $Y_{B2}$  face relatively large washout effect, still they generate sizable contribution and  $Y_{B3}$  gives sub-dominant contribution as shown in Fig.8. Here also we have plotted a contour between  $\text{Re}(x_D)$  and  $\lambda_2$ , assuming  $\text{Re}(x_C) = \text{Re}(x_D)$  with  $Y_B$  fixed at its central value, as shown in Fig.9 (right panel). We find that in this case, smaller values of  $\text{Re}(x_C) = \text{Re}(x_D)$  are favored compared to the ones in NH case.

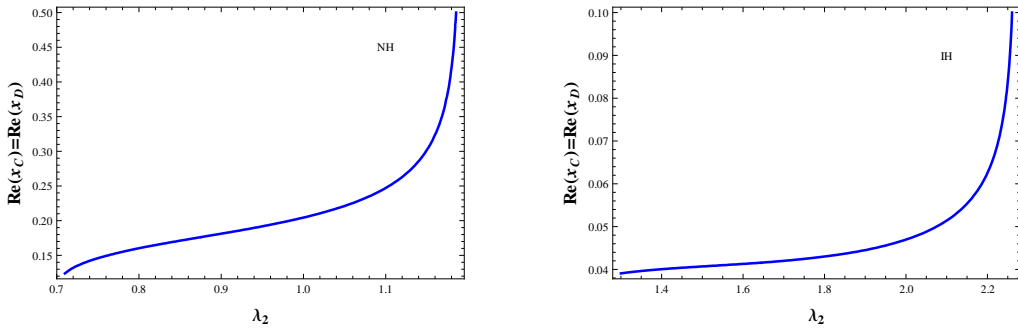


Figure 9: Contour plot of  $\text{Re}(x_C)(=\text{Re}(x_D))$  and  $\lambda_2$ , with  $Y_B$  fixed at its central value.

Since the RH Majorana neutrino masses (in IH case particularly) are close to each other, we need to check the possibility of satisfying condition for resonant leptogenesis [54]. In our

model, the quantity related to the mass degeneracy has been computed and found to be

$$\frac{M_2}{M_1} - 1 \approx (10^{-2} - 10^{-3}), \quad (5.10)$$

after scanning over the full range of  $\lambda_2$  ( $1.3 \lesssim \lambda_2 \lesssim 2.3$ ). We find that the resonance condition,

$$\left| \frac{M_2}{M_1} - 1 \right| \sim \left| \frac{(\hat{Y}_\nu \hat{Y}_\nu^\dagger)_{12}}{16\pi} \right|,$$

is not satisfied in our model. This is because the term in the right-hand-side of the resonance condition turns out to be of order  $5 \times 10^{-2} \kappa y [\text{Re}(x_C) \cos \theta + \text{Re}(x_D) \sin \theta]$ . As  $\kappa \sim 10^{-2}$ ,  $y \sim 10^{-1}$  and  $\theta$  is expected to produce correct  $\theta_{13}$ ,

$$\frac{(\hat{Y}_\nu \hat{Y}_\nu^\dagger)_{12}}{16\pi} \sim 10^{-5} - 10^{-6}.$$

Hence, in the present model, the resonant condition is not satisfied.

## 5.2 Leptogenesis with fixed $\lambda_2$ and varying $\lambda_1$

In this case we have taken a different approach by keeping  $\lambda_2$  fixed at certain value,  $\lambda_2 = 1$  for NH and  $\lambda_2 = 2.1$  for IH<sup>4</sup>. Then we can study the variation of  $Y_B$  with  $\lambda_1$ . The range of  $\lambda_1$  ( $0.33 \lesssim \lambda_1 \lesssim 0.41$ ) is of course restricted from Fig.1 in section 3. By using Eq.(4.1) and taking  $r = 0.03$ , we can now investigate the variation of  $\cos \phi_{ba}$  vs.  $\lambda_1$ . This is shown in

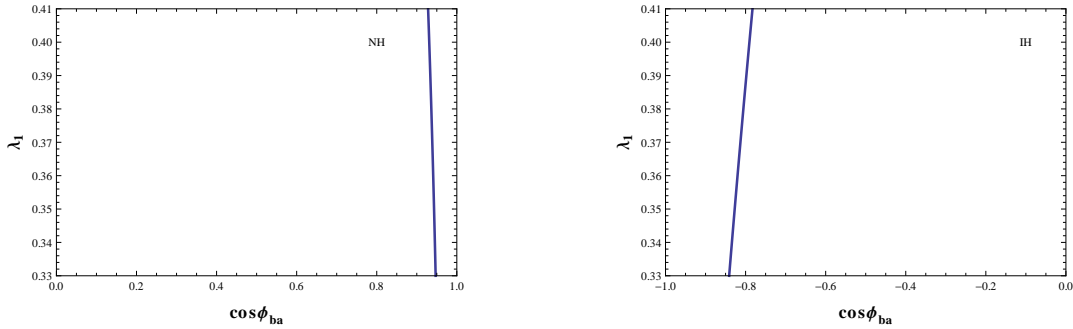


Figure 10:  $\cos \phi_{ba}$  vs  $\lambda_1$  for  $\lambda_2 = 1$  NH and  $\lambda_2 = 2.1$  for IH.

Fig.10. We find that  $\cos \phi_{ba}$  does not vary much with  $\lambda_1$  in the specified range. Similar to the one discussed in section 4, we can also set the Majorana phases  $\alpha_{21}$  and  $\alpha_{31}$  as a function of  $\lambda_1$  and finally we plot  $Y_B$  against  $\sin^2 \theta_{13}$  in Fig.11 as  $\sin^2 \theta_{13}$ 's dependence on  $\lambda_1$  is known. Note that, here also we have used the values  $\text{Re}(x_{C,D}) = 0.2$  for NH and 0.05 for IH as before. The maximum value of the effective neutrino mass parameter turns out to be  $|\langle m \rangle| \sim 0.01$  eV for NH (0.025 eV for IH).

---

<sup>4</sup>From Fig.3 and Planck limit on  $\sum m_i$ , note that there is no such common value of  $\lambda_2$  exists for which both NH and IH cases can be considered.

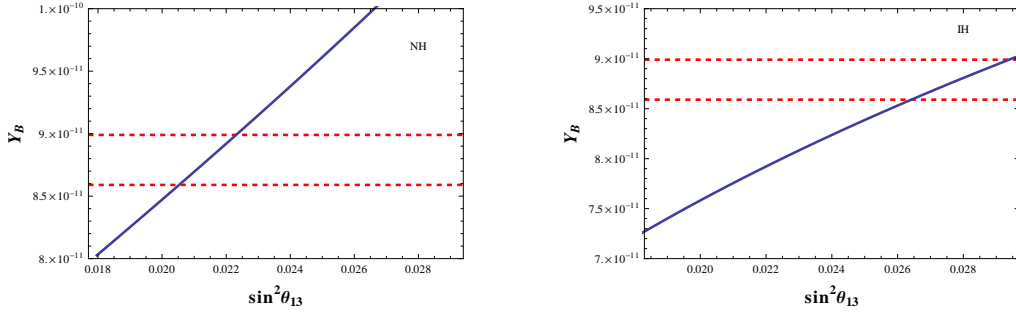


Figure 11: Baryon asymmetry  $Y_B$  vs  $\sin^2 \theta_{13}$  for NH (left panel) and IH (right panel). Here the region between horizontal dashed lines represent observed value for  $Y_B$  from [53].

## 6 Conclusion

In this work, we have studied the generation of nonzero  $\theta_{13}$  in a  $A_4$  symmetric framework. For this, we have extended the particle content of the AF model by adding one flavon,  $\xi'$ . In doing so, we consider the generation of light neutrino masses and mixing through the type-I see-saw mechanism. The addition of  $\xi'$  leads to a deformed structure for the right handed neutrino mass matrix as compared to the one obtained in case of tri-bimaximal mixing pattern. The explicit structure of the right handed neutrino mass matrix as well as the neutrino Yukawa matrices dictated by the flavor symmetry imposed ( $A_4 \times Z_3$ ), helps in studying the mixing angles involved in the  $U_{PMNS}$  matrix. We find that our framework can reproduce all the mixing angles consistent with recent experimental findings for a restricted range of parameter space for  $\lambda_1$  involved in the theory. We find a modified sum rule for this particular set-up. Also the effective neutrino mass parameter  $|\langle m \rangle|$  is studied. Since the structure of right handed neutrino sector is known, it also opens up the possibility to study leptogenesis in this framework and particularly the involvement of Majorana phases in the setup can be utilized. Following [27], we then study the Majorana phases  $\alpha_{21}$  and  $\alpha_{31}$  involved in  $U_{PMNS}$  and their dependence on parameter  $\lambda_2$ , while keeping  $\lambda_1$  fixed at a value that could reproduce the best fit value of  $\sin^2 \theta_{13}$ . This is done while constraints on neutrino parameters like the ratio of  $\Delta m_{21}^2$  and  $\Delta m_{31}^2$  is considered in conjugation with the sum rule obtained. It is known that this sort of model will not generate lepton asymmetry due to the special form of neutrino Yukawa matrix involved. The same conclusion holds here also and we need to consider the next-to-leading order effect to the neutrino Yukawa sector in order to realize nonzero lepton asymmetry. We have calculated the next-to-leading order terms in our setup and their involvement in the expression for the CP-asymmetry parameter  $\epsilon_i$ . Then we have shown that within ‘one flavor approximation’, our setup is able to generate sufficient amount of lepton asymmetry through the decay of the right handed neutrinos (and sneutrinos) without assigning large values to the parameters involved. In obtaining this result, we use the information obtained on the

Majorana phases  $\alpha_{21}, \alpha_{31}$  as function of the parameters involved. As the baryon asymmetry can be linked with the generated lepton asymmetry finally we have studied the variation of baryon asymmetry parameter  $Y_B$  with  $\lambda_2$ . The effect of having nonzero  $\theta_{13}$  is also studied.

It can also be noted that the framework restricts the RH neutrino masses in a narrow range between  $(1 + \tan^2 \beta)10^{12}$  GeV and  $10^{14}$  GeV as evident from the discussion below Eq.(5.8). This in turn can be used to estimate the scales involved in the theory. With our consideration that all the vevs of the new scalars involved in the set-up to be of similar order of magnitude,  $v$ , the RH neutrino masses are of order  $M_i \sim 2xv$  as seen from Eq.(3.9-3.11). With coupling constants  $x \sim \mathcal{O}(1)$ , it further tells that  $v$  is of order  $10^{13}$  GeV with  $\tan \beta \sim 3$ . Therefore the new flavons (whose masses are proportional to  $v$  as seen from Eq.(B.1)) are found to be as heavy as RH neutrinos, while the couplings involved are considered to be of order 1. So although the RH neutrinos have other interactions with the new scalars of the set-up (from Eq.(2.3)), its decay mode is essentially dominated by the Yukawa interactions with the lepton and higgs doublets only. This justifies our consideration of employing Eq.(5.1) which is the standard expression of leptogenesis for the decay of RH neutrinos through Yukawa interaction. Now, in order to produce correct amount of lepton asymmetry, we require to have  $\kappa = \frac{v}{\Lambda}$  to be of order  $10^{-2}$ . This value is also consistent with the tau lepton mass as appeared in Eq.(2.1) with the coupling  $y_\tau \sim \mathcal{O}(1)$ . This sets the typical value of the cut-off scale  $\Lambda$  to be  $10^{15}$  GeV. The close proximity of  $\Lambda$  with the grand unification scale turns out to be an intriguing feature of the model.

## Appendix

### A $A_4$ Multiplication Rules:

$A_4$  is discrete group of even permutation of four objects<sup>5</sup>. It has three inequivalent one-dimensional representation  $1, 1', 1''$  and a irreducible three dimensional representation  $3$ . Product of the singlets and triplets are given by

$$\begin{aligned}
1 \otimes 1 &= 1, \\
1' \otimes 1' &= 1'', \\
1' \otimes 1'' &= 1, \\
1'' \otimes 1'' &= 1', \& \\
3 \otimes 3 &= 1 \oplus 1' \oplus 1'' \oplus 3_A \oplus 3_S
\end{aligned} \tag{A.1}$$

---

<sup>5</sup>For a detailed discussion on  $A_4$ , see [32].

where subscripts  $A$  and  $S$  stands for “asymmetric” and “symmetric” respectively. If we have two triplets  $(a_1, a_2, a_3)$  and  $(b_1, b_2, b_3)$ , their products are given by

$$\begin{aligned}
1 &\sim a_1 b_1 + a_2 b_3 + a_3 b_2, \\
1' &\sim a_3 b_3 + a_1 b_2 + a_2 b_1, \\
1'' &\sim a_2 b_2 + a_3 b_1 + a_1 b_3, \\
3_S &\sim \begin{bmatrix} 2a_1 b_1 - a_2 b_3 - a_3 b_2 \\ 2a_3 b_3 - a_1 b_2 - a_2 b_1 \\ 2a_2 b_2 - a_1 b_3 - a_3 b_1 \end{bmatrix}, \\
3_A &\sim \begin{bmatrix} a_2 b_3 - a_3 b_2 \\ a_1 b_2 - a_2 b_1 \\ a_3 b_1 - a_1 b_3 \end{bmatrix}.
\end{aligned} \tag{A.2}$$

## B $A_4$ Vaccum Alignments:

In our model driving part of the LO superpotential, invariant under  $A_4 \times Z_3$  with  $R = 2$ , can be written as

$$w_d = M(\phi_0^T \phi_T) + g(\phi_0^T \phi_T \phi_T) + \phi_0^S (g_1 \phi_S \phi_S + g_2 \phi_S \xi + g_3 \phi_S \xi') + \xi_0 (g_4 \phi_S \phi_S + g_5 \xi \xi). \tag{B.1}$$

Equations which give vacuum structure of  $\phi_T$  are given by:

$$\begin{aligned}
\frac{\partial w}{\partial \phi_{01}^T} &= M\phi_{T1} + \frac{2g}{3} (\phi_{T1}^2 - \phi_{T2}\phi_{T3}) = 0, \\
\frac{\partial w}{\partial \phi_{02}^T} &= M\phi_{T1} + \frac{2g}{3} (\phi_{T2}^2 - \phi_{T1}\phi_{T3}) = 0, \\
\frac{\partial w}{\partial \phi_{03}^T} &= M\phi_{T1} + \frac{2g}{3} (\phi_{T3}^2 - \phi_{T1}\phi_{T2}) = 0.
\end{aligned} \tag{B.2}$$

Solution of these equations can be given by:  $\langle \phi_T \rangle = (v_T, 0, 0)$  where  $v_T = -\frac{3M}{2g}$ . Again, equations responsible for vacuum alignments of  $\phi_S$ ,  $\xi$  and  $\xi'$  are:

$$\begin{aligned}
\frac{\partial w}{\partial \phi_{01}^S} &= \frac{2g_1}{3} (\phi_{S1}^2 - \phi_{S2}\phi_{S3}) + g_2 \xi \phi_{S1} + g_3 \xi' \phi_{S3} = 0 \\
\frac{\partial w}{\partial \phi_{02}^S} &= \frac{2g_1}{3} (\phi_{S2}^2 - \phi_{S1}\phi_{S3}) + g_2 \xi \phi_{S3} + g_3 \xi' \phi_{S2} = 0 \\
\frac{\partial w}{\partial \phi_{03}^S} &= \frac{2g_1}{3} (\phi_{S3}^2 - \phi_{S1}\phi_{S2}) + g_2 \xi \phi_{S2} + g_3 \xi' \phi_{S1} = 0 \\
\frac{\partial w}{\partial \xi_0} &= g_4 (\phi_{S1}^2 + 2\phi_{S2}\phi_{S3}) + g_5 \xi \xi = 0
\end{aligned} \tag{B.3}$$



From these equations we obtain  $\langle \phi_S \rangle = (v_S, v_S, v_S)$ ,  $\langle \xi \rangle = u$  and  $\langle \xi' \rangle = u' \neq 0$  with  $v_s^2 = \frac{-g_5 u^2}{3g_4}$  and  $u' = \frac{-g_2 u}{g_3}$ . Note that NLO correction terms with  $1/\Lambda$  suppression involving  $\xi'$  in the superpotential  $w_d$  are absent and so the vevs of the flavon fields remain unchanged.

## References

- [1] Y. Abe *et al.* [DOUBLE-CHOOZ Collaboration], Phys. Rev. Lett. **108**, 131801 (2012) [arXiv:1112.6353 [hep-ex]].
- [2] F. P. An *et al.* [DAYA-BAY Collaboration], Phys. Rev. Lett. **108**, 171803 (2012) [arXiv:1203.1669 [hep-ex]]; F. P. An *et al.* [Daya Bay Collaboration], arXiv:1406.6468 [hep-ex].
- [3] J. K. Ahn *et al.* [RENO Collaboration], Phys. Rev. Lett. **108**, 191802 (2012) [arXiv:1204.0626 [hep-ex]].
- [4] K. Abe *et al.* [T2K Collaboration], Phys. Rev. Lett. **112**, 061802 (2014) [arXiv:1311.4750 [hep-ex]].
- [5] J. Beringer *et al.* [Particle Data Group Collaboration], Phys. Rev. D **86**, 010001 (2012).
- [6] S. Fukuda *et al.* [Super-Kamiokande Collaboration], Phys. Lett. B **539**, 179 (2002) [hep-ex/0205075]; Y. Ashie *et al.* [Super-Kamiokande Collaboration], Phys. Rev. D **71**, 112005 (2005) [hep-ex/0501064]. P. Adamson *et al.* [MINOS Collaboration], Phys. Rev. Lett. **106**, 181801 (2011) [arXiv:1103.0340 [hep-ex]]. T. Araki *et al.* [KamLAND Collaboration], Phys. Rev. Lett. **94**, 081801 (2005) [hep-ex/0406035].
- [7] T. Schwetz, M. A. Tortola and J. W. F. Valle, New J. Phys. **10**, 113011 (2008) [arXiv:0808.2016 [hep-ph]].
- [8] D. V. Forero, M. Tortola and J. W. F. Valle, arXiv:1405.7540 [hep-ph].
- [9] S. M. Bilenky, J. Hosek and S. T. Petcov, Phys. Lett. B **94**, 495 (1980); P. Langacker, S. T. Petcov, G. Steigman and S. Toshev, Nucl. Phys. B **282**, 589 (1987).
- [10] P. F. Harrison, D. H. Perkins and W. G. Scott, Phys. Lett. B **458**, 79 (1999) [hep-ph/9904297].
- [11] S. F. King and C. Luhn, Rept. Prog. Phys. **76**, 056201 (2013) [arXiv:1301.1340 [hep-ph]].
- [12] E. Ma, Phys. Rev. D **70**, 031901 (2004) [hep-ph/0404199].
- [13] G. Altarelli and F. Feruglio, Nucl. Phys. B **720**, 64 (2005) [hep-ph/0504165].

- [14] G. Altarelli and F. Feruglio, Nucl. Phys. B **741**, 215 (2006) [hep-ph/0512103].
- [15] K. S. Babu, E. Ma and J. W. F. Valle, Phys. Lett. B **552**, 207 (2003) [hep-ph/0206292]; B. Adhikary, B. Brahmachari, A. Ghosal, E. Ma and M. K. Parida, Phys. Lett. B **638**, 345 (2006) [hep-ph/0603059]; M. Honda and M. Tanimoto, Prog. Theor. Phys. **119**, 583 (2008) [arXiv:0801.0181 [hep-ph]].
- [16] B. Brahmachari, S. Choubey and M. Mitra, Phys. Rev. D **77**, 073008 (2008) [Erratum-ibid. D **77**, 119901 (2008)] [arXiv:0801.3554 [hep-ph]].
- [17] Y. Lin, Nucl. Phys. B **813**, 91 (2009) [arXiv:0804.2867 [hep-ph]]; S. F. King, Phys. Lett. B **675**, 347 (2009) [arXiv:0903.3199 [hep-ph]]; G. C. Branco, R. Gonzalez Felipe, M. N. Rebelo and H. Serodio, Phys. Rev. D **79**, 093008 (2009) [arXiv:0904.3076 [hep-ph]]; Y. Lin, Nucl. Phys. B **824**, 95 (2010) [arXiv:0905.3534 [hep-ph]]; D. Aristizabal Sierra, F. Bazzocchi, I. de Medeiros Varzielas, L. Merlo and S. Morisi, Nucl. Phys. B **827**, 34 (2010) [arXiv:0908.0907 [hep-ph]]; S. Morisi and E. Peinado, Phys. Rev. D **80**, 113011 (2009) [arXiv:0910.4389 [hep-ph]]; Y. H. Ahn and C. -S. Chen, Phys. Rev. D **81**, 105013 (2010) [arXiv:1001.2869 [hep-ph]]; J. Barry and W. Rodejohann, Phys. Rev. D **81**, 093002 (2010) [Erratum-ibid. D **81**, 119901 (2010)] [arXiv:1003.2385 [hep-ph]]; Y. H. Ahn, arXiv:1006.2953 [hep-ph]; I. de Medeiros Varzielas and L. Merlo, JHEP **1102**, 062 (2011) [arXiv:1011.6662 [hep-ph]]; Y. H. Ahn, H. -Y. Cheng and S. Oh, Phys. Rev. D **83**, 076012 (2011) [arXiv:1102.0879 [hep-ph]].
- [18] Y. Shimizu, M. Tanimoto and A. Watanabe, Prog. Theor. Phys. **126**, 81 (2011) [arXiv:1105.2929 [hep-ph]].
- [19] E. Ma and D. Wegman, Phys. Rev. Lett. **107**, 061803 (2011) [arXiv:1106.4269 [hep-ph]].
- [20] S. F. King and C. Luhn, JHEP **1109**, 042 (2011) [arXiv:1107.5332 [hep-ph]].
- [21] Y. H. Ahn, H. -Y. Cheng and S. Oh, Phys. Rev. D **84**, 113007 (2011) [arXiv:1107.4549 [hep-ph]]; S. Antusch, S. F. King, C. Luhn and M. Spinrath, Nucl. Phys. B **856**, 328 (2012) [arXiv:1108.4278 [hep-ph]]; G. -J. Ding and D. Meloni, Nucl. Phys. B **855**, 21 (2012) [arXiv:1108.2733 [hep-ph]]; S. F. King and C. Luhn, JHEP **1203**, 036 (2012) [arXiv:1112.1959 [hep-ph]]; Y. H. Ahn and H. Okada, Phys. Rev. D **85**, 073010 (2012) [arXiv:1201.4436 [hep-ph]]; G. C. Branco, R. Gonzalez Felipe, F. R. Joaquim and H. Serodio, Phys. Rev. D **86**, 076008 (2012) [arXiv:1203.2646 [hep-ph]]; Y. H. Ahn and S. K. Kang, Phys. Rev. D **86**, 093003 (2012) [arXiv:1203.4185 [hep-ph]]; H. Ishimori and E. Ma, Phys. Rev. D **86**, 045030 (2012) [arXiv:1205.0075 [hep-ph]].

- [22] G. Altarelli, F. Feruglio, L. Merlo and E. Stamou, JHEP **1208**, 021 (2012) [arXiv:1205.4670 [hep-ph]].
- [23] G. Altarelli, F. Feruglio and L. Merlo, Fortsch. Phys. **61**, 507 (2013) [arXiv:1205.5133 [hep-ph]]; E. Ma, A. Natale and A. Rashed, Int. J. Mod. Phys. A **27**, 1250134 (2012) [arXiv:1206.1570 [hep-ph]]; Y. H. Ahn, S. Baek and P. Gondolo, Phys. Rev. D **86**, 053004 (2012) [arXiv:1207.1229 [hep-ph]]; Y. BenTov, X. -G. He and A. Zee, JHEP **1212**, 093 (2012) [arXiv:1208.1062 [hep-ph]]; E. Ma, Phys. Rev. D **86**, 117301 (2012) [arXiv:1209.3374 [hep-ph]]; M. -C. Chen, J. Huang, J. -M. O'Bryan, A. M. Wijangco and F. Yu, JHEP **1302**, 021 (2013) [arXiv:1210.6982 [hep-ph]]; M. Holthausen, M. Lindner and M. A. Schmidt, Phys. Rev. D **87**, no. 3, 033006 (2013) [arXiv:1211.5143 [hep-ph]]; I. de Medeiros Varzielas and D. Pidt, JHEP **1303**, 065 (2013) [arXiv:1211.5370 [hep-ph]]; N. Memenga, W. Rodejohann and H. Zhang, Phys. Rev. D **87**, 053021 (2013) [arXiv:1301.2963 [hep-ph]]; S. Antusch, S. F. King and M. Spinrath, Phys. Rev. D **87**, no. 9, 096018 (2013) [arXiv:1301.6764 [hep-ph]]; S. F. King, S. Morisi, E. Peinado and J. W. F. Valle, Phys. Lett. B **724**, 68 (2013) [arXiv:1301.7065 [hep-ph]]; A. Kadosh, JHEP **1306**, 114 (2013) [arXiv:1303.2645 [hep-ph]]; M. Borah, B. Sharma and M. K. Das, arXiv:1304.0164 [hep-ph]; Y. H. Ahn, S. K. Kang and C. S. Kim, Phys. Rev. D **87**, no. 11, 113012 (2013) [arXiv:1304.0921 [hep-ph]]; S. F. King, Phys. Lett. B **724**, 92 (2013) [arXiv:1305.4846 [hep-ph]]; S. Antusch, C. Gross, V. Maurer and C. Sluka, Nucl. Phys. B **877**, 772 (2013) [arXiv:1305.6612 [hep-ph]]; S. Morisi, D. V. Forero, J. C. Romo and J. W. F. Valle, Phys. Rev. D **88**, no. 1, 016003 (2013) [arXiv:1305.6774 [hep-ph]]; P. M. Ferreira, L. Lavoura and P. O. Ludl, Phys. Lett. B **726**, 767 (2013) [arXiv:1306.1500 [hep-ph]]; S. Antusch and D. Nolde, JCAP **1310**, 028 (2013) [arXiv:1306.3501 [hep-ph]]; S. Antusch, C. Gross, V. Maurer and C. Sluka, Nucl. Phys. B **879**, 19 (2014) [arXiv:1306.3984 [hep-ph]]; Y. H. Ahn and S. Baek, Phys. Rev. D **88**, no. 3, 036017 (2013) [arXiv:1306.4138 [hep-ph]]; D. Borah, Nucl. Phys. B **876**, 575 (2013) [arXiv:1307.2426]; G. -J. Ding, S. F. King and A. J. Stuart, JHEP **1312**, 006 (2013) [arXiv:1307.4212]; A. E. Carcamo Hernandez, I. de Medeiros Varzielas, S. G. Kovalenko, H. Pas and I. Schmidt, Phys. Rev. D **88**, no. 7, 076014 (2013) [arXiv:1307.6499 [hep-ph]]; Y. Zhao and P. -F. Zhang, arXiv:1402.5834 [hep-ph]; Y. Grossman and W. H. Ng, arXiv:1404.1413 [hep-ph]; D. Aristizabal Sierra and I. de Medeiros Varzielas, JHEP **1407**, 042 (2014) [arXiv:1404.2529 [hep-ph]]; V. V. Vien and H. N. Long, arXiv:1405.4665 [hep-ph].
- [24] For a review, see S. Davidson, E. Nardi and Y. Nir, Phys. Rept. **466**, 105 (2008) [arXiv:0802.2962 [hep-ph]] and references there in.

- [25] E. E. Jenkins and A. V. Manohar, Phys. Lett. B **668**, 210 (2008) [arXiv:0807.4176 [hep-ph]].
- [26] I. K. Cooper, S. F. King and C. Luhn, Nucl. Phys. B **859**, 159 (2012) [arXiv:1110.5676 [hep-ph]].
- [27] C. Hagedorn, E. Molinaro and S. T. Petcov, JHEP **0909**, 115 (2009) [arXiv:0908.0240 [hep-ph]].
- [28] S. Pascoli, S. T. Petcov and A. Riotto, Phys. Rev. D **75**, 083511 (2007) [hep-ph/0609125].
- [29] S. Blanchet, P. Di Bari and G. G. Raffelt, JCAP **0703**, 012 (2007) [hep-ph/0611337].
- [30] S. Davidson, J. Garayoa, F. Palorini and N. Rius, JHEP **0809**, 053 (2008) [arXiv:0806.2832 [hep-ph]].
- [31] C. D. Froggatt and H. B. Nielsen, Nucl. Phys. B **147**, 277 (1979).
- [32] G. Altarelli and F. Feruglio, Rev. Mod. Phys. **82**, 2701 (2010) [arXiv:1002.0211 [hep-ph]].
- [33] B. Adhikary and A. Ghosal, Phys. Rev. D **78**, 073007 (2008) [arXiv:0803.3582 [hep-ph]]; S. -F. Ge, H. -J. He and F. -R. Yin, JCAP **1005**, 017 (2010) [arXiv:1001.0940 [hep-ph]].
- [34] G. Altarelli and D. Meloni, J. Phys. G **36**, 085005 (2009) [arXiv:0905.0620 [hep-ph]].
- [35] J. Barry and W. Rodejohann, Nucl. Phys. B **842**, 33 (2011) [arXiv:1007.5217 [hep-ph]]; S. F. King, A. Merle and A. J. Stuart, JHEP **1312**, 005 (2013) [arXiv:1307.2901 [hep-ph]].
- [36] S. -F. Ge, D. A. Dicus and W. W. Repko, Phys. Lett. B **702**, 220 (2011) [arXiv:1104.0602 [hep-ph]]; S. -F. Ge, D. A. Dicus and W. W. Repko, Phys. Rev. Lett. **108**, 041801 (2012) [arXiv:1108.0964 [hep-ph]]; D. Hernandez and A. Y. Smirnov, Phys. Rev. D **86**, 053014 (2012) [arXiv:1204.0445 [hep-ph]].
- [37] P. A. R. Ade *et al.* [Planck Collaboration], arXiv:1303.5076 [astro-ph.CO].
- [38] S. M. Bilenky and C. Giunti, Mod. Phys. Lett. A **27**, 1230015 (2012) [arXiv:1203.5250 [hep-ph]].
- [39] Y. Huang and B. -Q. Ma, arXiv:1407.4357 [hep-ph].
- [40] M. Fukugita and T. Yanagida, Phys. Lett. B **174**, 45 (1986).
- [41] M. Flanz, E. A. Paschos and U. Sarkar, Phys. Lett. B **345**, 248 (1995) [Erratum-ibid. B **382**, 447 (1996)] [hep-ph/9411366].

- [42] L. Covi, E. Roulet and F. Vissani, Phys. Lett. B **384**, 169 (1996) [hep-ph/9605319].
- [43] M. Plumacher, Z. Phys. C **74**, 549 (1997) [hep-ph/9604229].
- [44] W. Buchmuller and M. Plumacher, Phys. Lett. B **431**, 354 (1998) [hep-ph/9710460].
- [45] W. Buchmuller, P. Di Bari and M. Plumacher, Annals Phys. **315**, 305 (2005) [hep-ph/0401240].
- [46] G. F. Giudice, A. Notari, M. Raidal, A. Riotto and A. Strumia, Nucl. Phys. B **685**, 89 (2004) [hep-ph/0310123].
- [47] J. A. Harvey and M. S. Turner, Phys. Rev. D **42**, 3344 (1990).
- [48] G. Engelhard, Y. Grossman and Y. Nir, JHEP **0707**, 029 (2007) [hep-ph/0702151 [HEP-PH]].
- [49] G. Engelhard, Y. Grossman, E. Nardi and Y. Nir, Phys. Rev. Lett. **99**, 081802 (2007) [hep-ph/0612187].
- [50] S. T. Petcov, S. Profumo, Y. Takanishi and C. E. Yaguna, Nucl. Phys. B **676**, 453 (2004) [hep-ph/0306195].
- [51] S. T. Petcov, W. Rodejohann, T. Shindou and Y. Takanishi, Nucl. Phys. B **739**, 208 (2006) [hep-ph/0510404].
- [52] A. Djouadi and J. Quevillon, JHEP **1310**, 028 (2013) [arXiv:1304.1787 [hep-ph]].
- [53] C. L. Bennett *et al.* [WMAP Collaboration], Astrophys. J. Suppl. **208**, 20 (2013) [arXiv:1212.5225 [astro-ph.CO]].
- [54] A. Pilaftsis, Phys. Rev. D **56**, 5431 (1997) [hep-ph/9707235]; A. Pilaftsis and T. E. J. Underwood, Nucl. Phys. B **692**, 303 (2004) [hep-ph/0309342].